Memoirs of the Faculty of Engineering, Nagoya University
Vol. 27, No. 2. (1975)

MECHANISM OF FRACTURE AND FAILURE OF CONCRETE AS A COMPOSITE MATERIAL

YASUO TANIGAWA and YOSHIO KOSAKA

Department of Architecture

(Received October 31, 1975)

CONTENTS

1. General Introduction

Concrete is a multi-phase material consisted of several components, i. e., coarse aggregate, sand, unhydrated cement particles, cement gel, capillary and gel pores, pore water, entrapped and entrained air voids and so on[1)~3)]. However, it is apparent that concrete can be considered as a two-phase material in which a high volume fraction of coarse aggregate is uniformly distributed and embedded within a reasonably homogeneous mortar matrix. Such a two-phase model is acceptable as a first approximation as long as the dimensional level, at which the mechanical behavior is considered, is large compared with the maximum size of particles in matrix[2)].

The mechanical properties of concrete as a two-phase material are considerably affected by the properties and mix proportions of its components. Therefore, many investigators have attempted to make clear the effects of the properties of components and mix proportions on the mechanical properties of concrete[1)~5)]. However, most of the vast amount of available experimental data have been obtained from tests only at the engineering or phenomenological levels.

Generally, a knowledge of the internal structure of concrete is essential, if its complex mechanical behavior is to be properly understood. The basic mechanism of fracture and failure of concrete under load is the initiation and propagation of microscopic cracks which extend and interconnect until the whole internal structures are completely disrupted.

Therefore, there have been many attempts to measure the onset and propagation of microcracks by means of the methods as indicated in Table 1. 1[6)~55)]. In "Direct method" in Table 1. 1, the progressive microcracking in concrete is observed with a microscope or X-ray photographs. This method has an advantage that the mechanism of crack formation can be examined quantitatively, but has a disadvantage that long time and many efforts are required for observation. "Indirect method" is roughly subdivided into the following two groups: the acoustic method in which crack noise or the variation of ultra-sonic velocity transmitting in concrete due to microcracking are examined, and the method utilizing the stress-strain curve of concrete in which the state of internal microcracking is predicted in terms of the change of the external surface strain of test specimen. In these indirect methods, the measurement can be carried out more easily than that in the direct methods, but the information for microcracking obtained by such methods is rather unreliable. In the method of "Model analysis", two-phase model concretes consisted of idealized coarse aggregate and mortar matrix are used to help the understanding of the mechanism of fracture and failure of concrete. This method is also suitable for the fundamental recognition of the interaction of aggregate and matrix on the mechanical properties of concrete.

Table 1. 1. Previous studies on fracture and failure of concrete.

Classification		Investigators
Direct method	Observation by microscopy	Hsu・Slate・Sturman・Winter (1963)[6], Shah・Slate (1965)[7], Sturman・Shah・Winter (1965)[8], Yokomichi・Matsuoka・Takada (1966)[9], Hansen (1968)[10], Krishnaswamy (1968)[11], Meyers・Slate・Winter (1969)[12], Popovics (1969)[13], Shah・Chandra (1970)[14], Niwa・Koyanagi・Nakagawa (1971)[15], Kato (1971)[16], Yoshimoto・Kawakami (1972)[17], Amasaki・Akashi (1973)[18], Kosaka・Tanigawa (1974)[19][20]
	Observation by X-ray	Hsu・Slate・Sturman・Winter (1963)[6], Slate・Olsefski (1963)[21], Shah・Slate (1965)[7], Robinson (1965)[22], Liu・Nilson・Slate (1972)[23]
Indirect method	Observation by ultrasonic pulse velocity	Jones・Kaplan (1957)[24], Robinson (1965)[22], Jones (1965)[25], Shah・Chandra (1970)[14], Kawakami (1971)[26], Kato (1972)[27]
	Observation by crack noise	L' Hermite (1954)[28], Rüsch (1959)[29], Robinson (1965)[22], Yokomichi・Matsuoka・Takada (1966)[9]
	Observation by stress-strain curve	Brandtzaeg (1929)[30], Kaplan (1963)[31], Desayi・Viswanatha (1967)[32], Béres (1967)[33], Shah・Chandra (1968)[34], Yokomichi・Kakuta・Ayuta・Terasawa(1969)[35][36], Okamoto・Yamamoto (1971)[37], Kato (1972)[27], Hasaba・Kawamura (1972)[38], Kosaka・Tanigawa (1973)[39][40], Okushima・Suzuki・Nakatsuka (1973)[41], Yoshimoto・Kawakami (1974)[42]
Model analysis	Model with an aggregate	Shah・Winter (1968)[43], Yokomichi・Kakuta・Terasawa (1970)[36], Kosaka・Tanigawa・Oota (1971)[44][45], Shiire (1972)[46]
	Model with regularly arranged aggregates	Johoji・Kato (1957)[47], Fein (1971)[48], Buyukozturk・Nilson・Slate (1971)[49], Kosaka・Tanigawa・Oota (1972)[50][51], Okushima・Suzuki・Nakatsuka (1972)[52], Wischers・Lusche (1972)[53]
	Model with randomly arranged aggregates	Okajima (1970)[54], Kosaka・Tanigawa・Oota (1971)[55], Liu・Nilson・Slate (1972)[23]

Despite of many works on the observation of microcracking of concrete, there is still much that is not known of the effect of aggregate and matrix on the mechanism of fracture and failure of concrete as a two-phase composite material.

The main purpose of the present investigation is to make clear the effect of aggregate on the mechanism of fracture and failure of concrete at both the phenomenological and the structural levels, and the above three approaches are adopted for the investigation.

2. Progressive Microcracking in Concrete

2. 1. Introduction

The purpose of this chapter is to examine the effect of the type of coarse aggregate and the water-cement ratio of mortar matrix on the progressive microcracking in concrete. The direct method described in Chapter 1 was applied for observation of microcracks in concrete.

A series of experimental investigations have been conducted at Cornell University to examine the fracture process of concrete. Namely, Hsu, Sturman, Slate and Winter[6] have pointed out that; 1) bond cracks between mortar matrix and aggregate particles are present even before loading (which are termed "potential bond cracks" in the present paper), 2) the potential bond cracks propagate at the load larger than about 30 percent of ultimate, and 3) mortar cracks initiate at the load of about 70 percent of ultimate. But in their investigation, the extent of mortar cracks parallel to the loading axis has not been observed. Sturman, Shah and Winter[8] have examined the effect of flexual stress gradients on the internal crack propagation in concrete. Meyers, Slate and Winter[12] have examined the effect of long-time sustained loading. Moreover, Shah and Chandra[14] have made clear the relation between the fatigue strength of concrete and the internal crack propagation, and Krishnaswamy[11] have observed the progressive microcracking in concrete under uniaxial and triaxial compression.

In Japan, on the other hand, Niwa, Kobayashi, Koyanagi and Nakagawa[15] have carried out the uniaxial and triaxial compressive tests of normal concrete and suggested that the potential bond cracks are present beneath the coarse aggregate particles even before loading and that the ratio of the total length of bond cracks to that of interface between mortar matrix and coarse aggregate increases with increasing lateral pressure. Kato[16] has found that the amount of bond cracks and mortar cracks occupys about 97 percent among that of total cracks in concrete and that the amount of mortar cracks is of the order of 60 to 70 percent of that of bond cracks. Amasaki and Akashi[18] have investigated the crack propagation of concrete under impact loading.

As described above, many investigators have already reported the mechanism of microcracking and the fracture process of normal concrete but hardly reported the effect of the mechanical properties of mortar matrix and aggregate on them. Consequently, the effect of the qualities of coarse aggregate and mortar matrix on the progressive microcracking in normal and artificial lightweight aggregate concretes was primarily examined in the present chapter. While, the direct method as used in this chapter requires a relatively long time for observation of microcracks. Therefore, the correlation between the internal microcracking in concrete and the changes of external surface strain of concrete was also examined in the present chapter. By applying these results, more detailed examination for the effect of variables related to aggregate such as the type, size and volume fraction will be made in the next chapter.

2. 2. Test procedure

2. 2. 1. Outline of experiments

The following two kinds of experiment were performed in the present chapter.

The outline of experiments is shown in Table 2. 1.

1) Experiment-Ⅱ. 1; Cylindrical specimens with 10 cm in diameter and 20 cm in height were compressed uniaxially up to each of the preselected stresses of about 30, 50, 70, 90 or 100 percent of the compressive strength. After unloaded, the specimens were cut by a diamond blade saw in the plane parallel to the longitudinal axis and the state of internal microcracks was observed directly with a stereoscopic microscope.

2) Experiment-Ⅱ. 2; In Exp.-Ⅱ. 1, the process of microcracking up to the failure of an identical specimen can not been examined continuously, since the specimen is unloaded and cut immediately after the load is reached to a certain value. Accordingly, plate specimens of 15×1 cm in cross section and 15 cm in height fabricated by cutting from prismatic concrete specimens of 15×15 cm in section and 53 cm in length were used in Exp.-Ⅱ. 2. The uniaxial load was applied continuously up to the failure of specimen by the method as shown in Fig. 2. 1 and the progressive microcracking in the specimen was observed with a microscope. The primary reason why the specimen of 1 cm thickness was used is to examine mainly bond cracks at the interface between mortar matrix and all coarse aggregates (particle size =10−15 mm) and to obtain as nearly as possible a state of plane stress.

Table 2. 1. Outline of experiments.

Notation of experiment	Notation of specimen	Size of specimen (cm)	Materials used			W/C	V_{sa}/V_c	V_{ca}/V_{cc}	ϕ_a (mm)
			Cement	Fine aggregate	Coarse aggregate				
Exp.-Ⅱ.1	CC-NA	ϕ 10×20	Ordinary Portland cement	River sand	NA	0.35	0.88	0.30	10-15
	CC-NA				NA	0.65	3.15	0.30	10-15
	CC-LC				LC	0.35	0.88	0.30	10-15
	CC-LC				LC	0.65	3.15	0.30	10-15
Exp.-Ⅱ.2	SC-NA	15×15×1	Ordinary Portland cement	River sand	NA	0.45	2.50	0.30	10-15
	SC-NA				NA	0.55	2.50	0.30	10-15
	SC-NA				NA	0.70	2.50	0.30	10-15
	SC-LC				LC	0.55	2.50	0.30	10-15

[Notation] W/C: Water-cement ratio, V_{sa}/V_c: Sand-cement ratio, ϕ_a: Size range of coarse aggregate, NA: River gravel, LC: Artificial lightweight aggregate (coated type).

2. 2. 2. Fabrication of specimen and mechanical properties of concrete

(1) Materials used

Ordinary Portland cement (compressive strength at the age of 28 days=408 kg/cm^2), Kiso-river sand and gravel, and artificial lightweight coarse aggregate of coated type were prepared for concrete. The particle size of coarse aggregate was kept to 10-15 mm to eliminate the effect of the grading of aggregate. The physical properties of aggregate used in the experiments are shown in Table 2. 2.

(2) Fabrication and mechanical properties of concrete

Water-cement ratios (W/C) were 0. 35 and 0. 65 in Exp.-Ⅱ. 1, and 0. 45, 0. 55 and 0. 70 in Exp.-Ⅱ. 2 by weight, respectively. The volume fraction of coarse

Table 2. 2. Properties of aggregates used.

Type	Size range (mm)	Specific gravity	Fineness modulus	Bulk density (kg/m³)	Water absorption (%)
River sand	0-2.5	2.63	1.99	1740	2.1
River gravel	10-15	2.56	7.00	1560	0.6
Lightweight aggregate	10-15	1.35	7.00	859	8.2

aggregate in concrete (V_{ca}/V_{cc}) was kept to 0.3 through Exp.-Ⅱ. 1 and Exp.-Ⅱ. 2. After remolded at the age of 2 days, the specimens were cured in water of a temperature of 20°±1°C until the tests. All tests were carried out at the age of 28 days. The plate specimens in Exp.-Ⅱ. 2 were fabricated by cutting from the comparable prismatic specimens at the age of 25 days. The number of test specimens was eighty in both Exp.-Ⅱ. 1 and Exp.-Ⅱ. 2.

Table 2. 3 shows the compressive strength (F_{cc}), tensile splitting strength (F_{tc}), secant modulus (E_c) and Poisson's ratio (ν_c) at a stress level of one-third the compressive strength obtained by cylindrical concrete specimens at the age of 28 days.

Table 2. 3. Quality of concrete.

Notation of experiment	Notation of specimen	W/C	F_{cc} (kg/cm²)	F_{tc} (kg/cm²)	E_c (kg/cm²)	ν_c
Exp.-Ⅱ.1	CC-NA	0.35	550	33.2	3.65×10^5	0.21
	CC-NA	0.65	242	21.3	2.40×10^5	0.20
	CC-LC	0.35	430	28.0	2.12×10^5	0.17
	CC-LC	0.65	241	20.5	1.65×10^5	0.20
Exp.-Ⅱ.2	SC-NA	0.45	382	29.7	2.78×10^5	0.24
	SC-NA	0.55	306	25.6	2.46×10^5	0.20
	SC-NA	0.70	198	18.2	1.92×10^5	0.18
	SC-LC	0.55	263	22.0	1.76×10^5	0.18

2. 2. 3. Methods of loading and measurement

All specimens were concentrically loaded in the direction parallel to casting by a hydraulic testing machine. The loading rate was kept to 2-3 kg/cm²/sec. in accordance with the specification of JIS A 1108.

The detail of the loading method of each experiment is as follows:

1) Exp.-Ⅱ. 1; Five cylindrical specimens were first loaded up to failure and the stress (σ)-strain (ε) curve and the compressive strength (F_{cc}) of concrete were obtained. Next, three specimens were loaded up to each of the preselected stresses of about 30, 50, 70 or 90 percent of the compressive strength and unloaded. Immediately after unloaded, the specimens were cut parallel to the loading axis by a diamond blade. The non-loaded specimens were also prepared to examine the

state of potential bond cracks.

2) Exp.-Ⅱ. 2; A device for loading shown in Fig. 2. 1 was used in Exp.-Ⅱ. 2 to prevent the overturn of specimen during the compressive loading. As it was anxious that the secondary stress would be induced in the specimen by this device, the strain in a bolt (B shown in Fig. 2. 1) was measured up to the failure of specimen, but was negligible. Accordingly, it was considered that the behavior of specimen did not been changed by using this device. In Exp.-Ⅱ. 2, lubricating pads consisted of 0. 3 mm thick rubber sheet and 0. 1 mm thick aluminium sheet with lubricated surface by silicon grease were inserted between the ends of specimen and the loading platens to minimize the effect of restraint at the ends. The coefficient of friction between the ends and the loading platens in this case was about 0. 005.

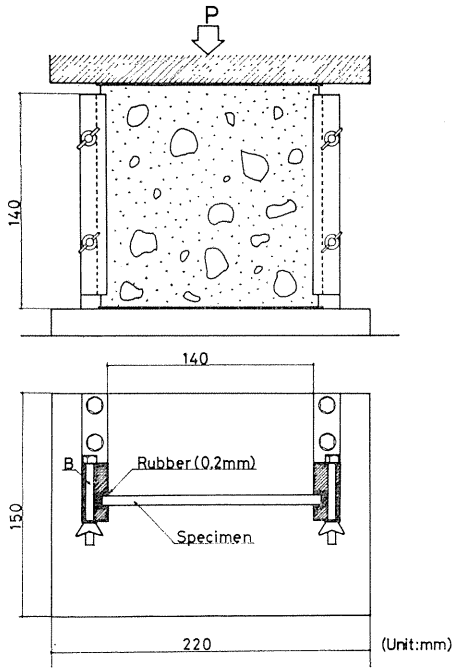

Fig. 2. 1. Loading device used in Exp. -Ⅱ. 2.

(2) Observation of microcracks

The method for observation of microcracks in Exp.-Ⅱ. 1 was as follows:

① After unloaded, the specimen was cut by a diamond blade saw. ② The saw-cut surface was washed by water and allowed to dry for approximately 2 hours. ③ The surface was painted with red ink and polished by carborundum powders. ④ Microcracks penetrated with red ink were observed by a stereoscopic microscope and the naked eyes.

In Exp.-Ⅱ. 2, the surface of specimen was painted thinly with red ink before loading and the progressive microcracking was continuously observed up to the failure of specimen with a microscope.

(3) Measurement of strains

1) Exp.-Ⅱ. 1; The longitudinal strain (ε_y) and the circumferential strain (ε_x)

were measured by 67 mm length wire strain gages attached to the center of cylinder. The volumetric strain ($\varepsilon_v=\varepsilon_y-2\varepsilon_x$) and Poisson's ratio ($\nu_c=\varepsilon_x/\varepsilon_y$) were calculated from the measured values of ε_x and ε_y.

2) Exp.-Ⅱ. 2; 67 mm length wire strain gages were used for the measurement of average strains in the longitudinal axis (y-direction) and the lateral axis (x-direction) and 5 mm length wire strain gages were used for the measurement of local strains in mortar matrix, coarse aggregate and interface between them, respectively.

2. 3. Test results and discussion

2. 3. 1. Relation between progressive microcracking and qualities of coarse aggregate and mortar matrix

In the present clause, the effect of qualities of coarse aggregate and mortar matrix on the type, extent, location and progress of microcracks obtained by Exp.-Ⅱ. 1 will be discussed.

(1) Initiation and propagation of microcracks

Typical examples of the state of microcracking in normal and lightweight aggregate concretes are shown in Photos. 2. 1 and 2. 2, respectively.

1) Type of microcracks; The type of microcracks observed in normal concrete is roughly classified to mortar cracks formed approximately parallel to the loading axis and bond cracks at the interface between mortar matrix and coarse aggregate, as shown in Photo. 2. 1. Few aggregate cracks were observed in normal concrete. On the other hand, the type of microcracks observed in lightweight aggregate concrete varied with the water-cement ratio of mortar matrix. For $W/C=0.65$, few aggregate cracks were observed in a manner similar to normal concrete, but for

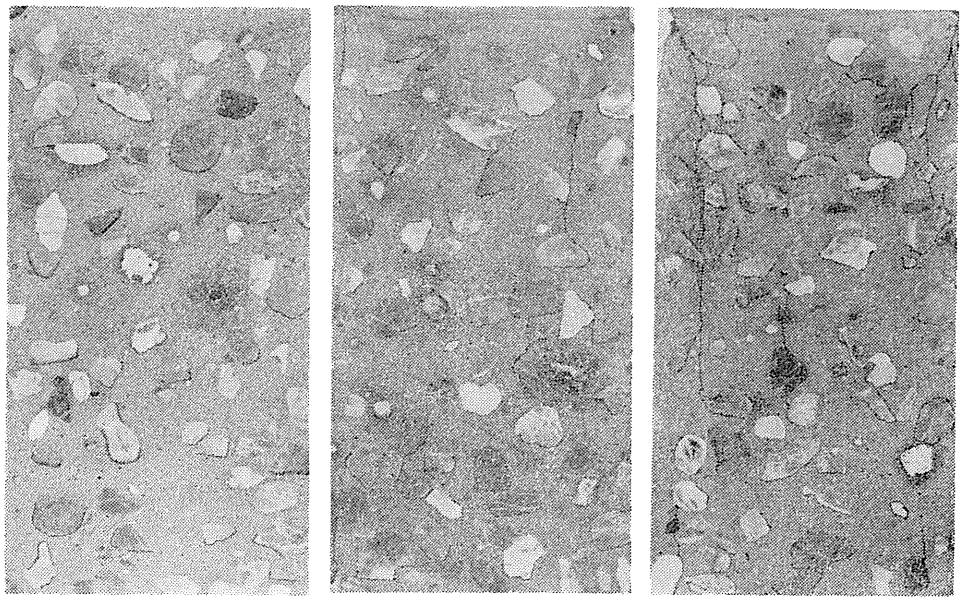

Photo. 2. 1. 1. $\sigma/F_{cc}=0$ Photo. 2. 1. 2. $\sigma/F_{cc}\fallingdotseq 0.7$ Photo. 2. 1. 3. $\sigma/F_{cc}=1.0$

Photo. 2. 1. Microcracking in normal concrete.

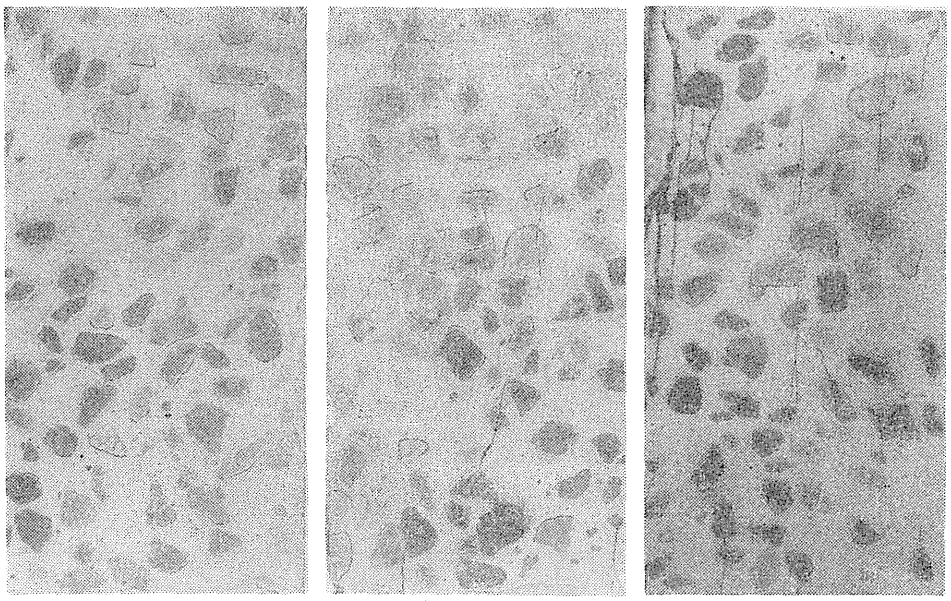

Photo. 2. 2. 1. $\sigma/F_{cc}=0$ Photo. 2. 2. 2. $\sigma/F_{cc}\fallingdotseq 0.7$ Photo. 2. 2. 3. $\sigma/F_{cc}=1.0$

Photo. 2. 2. Microcracking in lightweight aggregate concrete.

$W/C=0.35$, many cracks propagated in aggregate particles approximately parallel to the loading axis.

2) Extent of microcracks; Next, the process of progressive microcracking will be discussed in detail for each of the preselected stress levels (σ) expressed in terms of the compressive strength of concrete (F_{cc}).

i) In the case of $\sigma/F_{cc}=0$; According to Photos. 2. 1. 1 and 2. 2. 1 showing the state of potential cracks before loading, most of the potential cracks were present beneath the coarse aggregate particles and the amount of potential cracks present in the upper half of specimen was slightly more than that in the lower half, regardless of the type of coarse aggregate used. Cracks owing to drying shrinkage were hardly observed, since all specimens in Exp.-Ⅱ. 1 were cured in water. Consequently, it was concluded that most of potential cracks were weak porous mortar regions resulted from bleeding in concrete.

ii) In the case of $\sigma/F_{cc}\fallingdotseq 0.3$; The extent of microcracking at about 30 percent relative stress was approximately consistent with that in non-loaded specimens. Accordingly it was considered, regardless of the qualities of mortar matrix and coarse aggregate, that the microcracks in concrete would never occur or propagate at the stress level smaller than about 30 percent of ultimate.

iii) In the case of $\sigma/F_{cc}\fallingdotseq 0.5$; New bond cracks occurred not only at the bottom surface but also at the top surface of coarse aggregate and potential bond cracks beneath the coarse aggregate particles began to propagate at this stage, independently of the quality of concrete. Several bond cracks propagated around coarse aggregate particles with a small saw-cut section and a few mortar cracks were observed in only the normal concrete with $W/C=0.65$.

iv) In the case of $\sigma/F_{cc}\fallingdotseq 0.7$; At this loading stage, the amount of bond cracks increased rapidly as shown in Photos. 2. 1. 2 and 2. 2. 2, regardless of the type and quality of concrete. Mortar cracks bridged from bond cracks were ob-

served in normal and lightweight aggregate concretes, except for lightweight aggregate concrete with $W/C=0.65$. For lightweight aggregate concrete with $W/C=0.35$, a few aggregate cracks propagated approximately parallel to the loading axis. While, there was no aggregate crack and mortar crack at this stress level for lightweight aggregate concrete with $W/C=0.65$.

v) In the case of $\sigma/F_{cc}\fallingdotseq 0.9$; The amount of bond cracks and mortar cracks increased more rapidly at this stress level, except for lightweight aggregate concrete with $W/C=0.65$. Mortar cracks bridged between bond cracks or aggregate cracks to form the long continuous crack patterns and the side of cylindrical specimen spalled out in a few lightweight aggregate concretes with $W/C=0.35$. For lightweight aggregate concrete with $W/C=0.65$, mortar cracks began to propagate initially at this stress level.

vi) In the case of $\sigma/F_{cc}=1.0$; As shown in Photos. 2. 1. 3 and 2. 2. 3, the extent of microcracking at the failure of specimen was different from the strength of mortar matrix. For concretes with $W/C=0.65$, sliding planes due to the restraint from friction between the loading platens and the ends of specimen were formed at the ends of specimen and were bridged between the continuous cracks in the central

Table 2. 4. Fracture process of concrete (Experiment-Ⅱ.1).

Notation of specimen		CC-NA		CC-LC	
W/C		0.35	0.65	0.35	0.65
σ/F_{cc}	0	Potential bond crack at the bottom surface of coarse aggregate	Potential bond crack at the bottom surface of coarse aggregate	Potential bond crack at the bottom surface of coarse aggregate	Potential bond crack at the bottom surface of coarse aggregate
	0.3	Similar to $\sigma/F_{cc}=0$	Similar to $\sigma/F_{cc}=0$	Similar to $\sigma/F_{cc}=0$	Similar to $\sigma/F_{cc}=0$
	0.5	Initial propagation of bond crack	Initial propagation of bond crack Initiation of a few mortar cracks	Initial propagation of bond crack	Initial propagation of bond crack
	0.7	Initiation of mortar crack	Initiation of mortar crack	Initiation of mortar crack and aggregate crack	Propagation of bond crack
	0.9	Interconnection of mortar crack to bond crack	Interconnection of mortar crack to bond crack	Interconnection of mortar crack to aggregate crack	Initiation of mortar crack and interconnection of it to bond crack
	1.0	Initiation of long continuous crack and of a few aggregate cracks	Shear failure in the top zone of specimen	Initiation of long continuous crack	Shear failure in the top and bottom zone of specimen

portion. For concretes with $W/C=0.35$, on the other hand, many struts due to the axially continuous cracks were formed parallel to the loading axis.

Table 2. 4 shows the outline of the progressive microcracking in normal and lightweight aggregate concretes as described above.

(2) Length, width and inclination of microcracks

In this clause, the effect of the type of coarse aggregate and the strength of mortar matrix on the internal fracture process of concrete will be examined in more detail, by using the measured values of the length, width and inclination angle of microcracks.

1) Length of microcracks; The relative length of microcracks in the unit area (l/A) is plotted in Figs. 2. 2. 1 and 2. 2. 2 against the ratio of the loading stress (σ) to the compressive strength of concrete (F_{cc}). The notations of b, m and a in these figures represent bond crack, mortar crack and aggregate crack, and CC-NA and CC-LC represent normal concrete and lightweight aggregate concrete, respectively. As shown in Figs. 2. 2. 1 and 2. 2. 2, the relative length of bond crack (l_b/A) is approximately constant for each of concretes at the ratio σ/F_{cc} smaller than about 0.5. That value becomes larger with the increasing value of W/C or the bleeding of concrete. At the stress level larger than 70 percent of the compressive strength, mortar cracks were formed in concretes, except for lightweight aggregate concrete with $W/C=0.65$ and aggregate cracks were also occurred in lightweight aggregate concrete with $W/C=0.35$, as described above. At the stress level larger than about 90 percent of ultimate, the rate of increase of bond cracks decreased compared with that before, but mortar and aggregate cracks increased rapidly with the relative stress level.

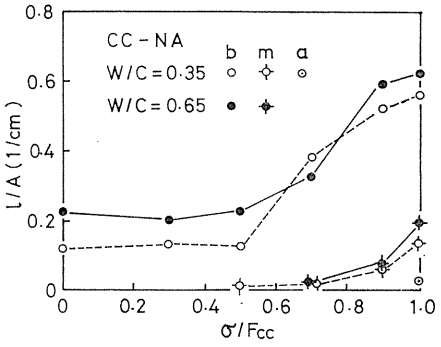

Fig. 2. 2. 1. Normal concrete

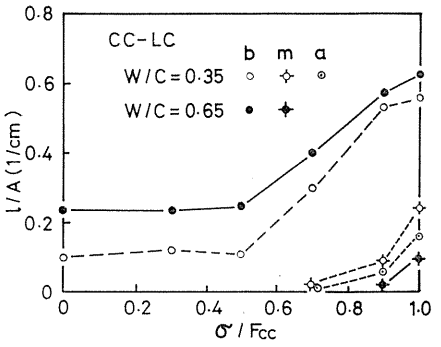

Fig. 2. 2. 2. Lightweight aggregate concrete

Fig. 2. 2. Relation between length of microcrack (l) and relative amount of stress (σ/F_{cc}).

2) Maximum width of microcracks; The width of microcracks represents the degree of internal structural changes of concrete, and is closely related to the change in Poisson's ratio due to loading and the durability of concrete. The relation between the maximum width of bond cracks (W_b) and the relative stress level (σ/F_{cc}) is indicated in Fig. 2. 3. As shown in Fig. 2. 3, the width of bond cracks (W_b) decreases slightly with the increase of relative stress level (σ/F_{cc}) at the ratio σ/F_{cc} smaller than about 0.5. The maximum width of bond cracks varies

considerably with the water-cement ratio of concrete. Namely, the maximum width of bond cracks for concretes with $W/C=0.65$ is about two times that for concretes with $W/C=0.35$. At the stress level larger than 50 percent of ultimate, the value of W_b for concretes with $W/C=0.35$ begins to increase but for a few specimens with $W/C=0.65$, the value of W_b decreases slightly by the compressive loading.

Ash[56] has observed that the width of weak layer of mortar beneath the coarse aggregate particles is approximately 100 micron and Krishnaswamy[11] has shown that the width of potential bond cracks is about 75 micron, regardless of the water-cement ratio. Whereas, the results in Exp.-Ⅱ. 1 differed from the aboves. This difference may be resulted from that the volume fraction and maximum size of coarse aggregate used in Exp.-Ⅱ. 1 were smaller than those used in Ash's or Krishnaswamy's experiments. Therefore, the degree of bleeding beneath the coarse aggregate particles in Exp.-Ⅱ. 1 was probably smaller than that in their experiments.

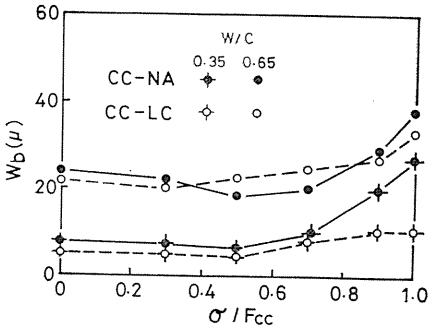

Fig. 2. 3. Relation between maximum width of bond crack (W_b) and relative amount of stress (σ/F_{cc}).

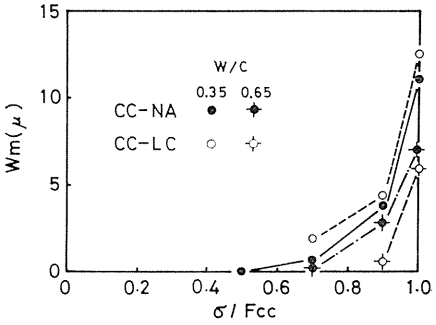

Fig. 2. 4. Relation between maximum width of mortar crack (W_m) and relative amount of stress (σ/F_{cc}).

Fig. 2. 4 shows the relation between the maximum width of mortar cracks (W_m) and the relative stress level (σ/F_{cc}). The maximum width of mortar cracks (W_m) for lightweight aggregate concrete with $W/C=0.35$ and for normal concrete increases rapidly with the relative stress level, in the range of σ/F_{cc} beyond about 0.7. However, this value is considerably smaller than the width of bond cracks at the same relative stress level.

The width of aggregate cracks occurred in lightweight aggregate concrete with $W/C=0.35$ was nearly equal to the width of its mortar cracks as in Fig. 2. 4, because most of aggregate cracks bridged between mortar cracks to form the continuous cracks.

3) Angle of inclination of bond cracks; Several investigators have pointed out that the fracture process and the compressive strength of concrete are significantly affected by the surface texture of coarse aggregate, i. e., the bond properties between coarse aggregate and mortar matrix. However, there is no available method at present to obtain directly the bond strength of river gravel or artificial lightweight aggregate in concrete, as their particle shapes are irregular and granular.

On the other hand, the measurement of the angle of inclination of bond cracks presents some available information for the bond properties between coarse aggregate and mortar matrix. Accordingly, the angle of inclination of bond cracks was

measured by the following method: ① The saw-cut surface of a coarse aggregate particle was devided into twenty-four fan-shaped parts with a vertical angle of 15 deg. ② The interface between coarse aggregate particle and mortar matrix in each fan-shaped partition was regarded as a straight line. ③ The angle (θ) of inclination of the straight line to x-direction in Fig. 2. 5 was measured. In such a case that there is a corner in a partition as shown by a point A in Fig. 2. 5, the angle of inclination of the longer interface in the partition was adopted.

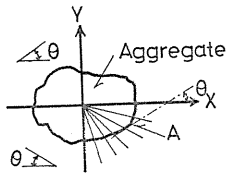

Fig. 2. 5. Method for measurement of inclination angle (θ) of bond crack.

Fig. 2. 6. 1 shows the frequency of the angle (θ) of potential bond cracks, where, the ordinate of Fig. 2. 6. 1 represents the ratio of the number of measured angle at each 10 deg. to the total number of measured angles. The frequency of θ of potential bond cracks is largest in the range of θ from 0 to 10 deg., independently of the type of coarse aggregate and the water-cement ratio, as shown in Fig. 2. 6. 1. This was resulted from that the potential cracks are usually present beneath the coarse aggregate particles.

The frequency of θ at the failure of specimen is given in Fig. 2. 6. 2, where, the ordinate represents the ratio of the number of measured angle at each 10 deg. subtracted by the number of θ of potential cracks in Fig. 2. 6. 1 to the total number of measured angles, that is, the frequency of the angle of bond cracks occurred newly under the compressive loading. As shown in Fig. 2. 6. 2, the frequency of θ at the failure of specimen is largest at $\theta \fallingdotseq 70$ deg. for concretes with $W/C=0.35$ and at $\theta \fallingdotseq 60$ deg. for concretes with $W/C=0.65$, independently of the type of coarse aggregate used.

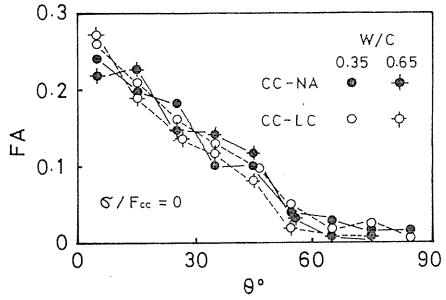

Fig. 2. 6. 1. In the case of $\sigma/F_{cc}=0$

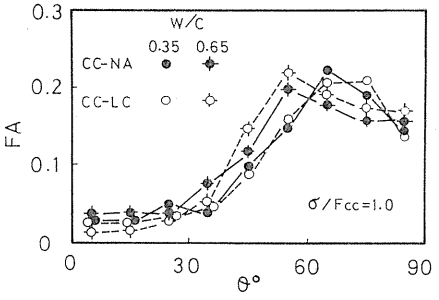

Fig. 2. 2. 2. In the case of $\sigma/F_{cc}=1.0$

Fig. 2. 6. Frequency of inclination angle of bond crack.

By using the above results, some information for the aggregate-matrix bond can be obtained. When the compressive stress (σ_c) is applied concentrically to the specimen as shown in Fig. 2. 7 (a), normal stress (σ_n) and tangential stress (τ_n) occur at the interface as shown in Fig. 2. 7 (b). If it is assumed that the bond crack will occur at the interface when a Mohr's stress circle shown in Fig. 2. 7 (b)

comes in contact with the straight line represented by Eq. (2. 1), the angle of friction (ϕ) in Eq. (2. 1) can be related to the angle of inclination of bond crack (θ) by Eq. (2. 2).

$$\tau = c - \tan\phi \cdot \sigma \tag{2. 1}$$

$$\phi = 2\theta - 90° \tag{2. 2}$$

where, c : cohesion ϕ : angle of friction
τ : shear stress σ : normal stress

As described above, the frequency of θ at the failure of specimen was largest at $\theta \fallingdotseq 70$ deg. and 60 deg. for concretes with $W/C = 0.35$ and 0.65, respectively. Therefore, it could be evaluated that the angles of friction (ϕ) were about 50 deg. and 30 deg. for concretes with $W/C = 0.35$ and 0.65, respectively, and the larger the smaller the water-cement ratio.

Since the state of internal stress in real concrete is never uniaxial as shown in Fig. 2. 7 (a), the results obtained from such a simplified model as described above are not necessarily applicable to real concrete.

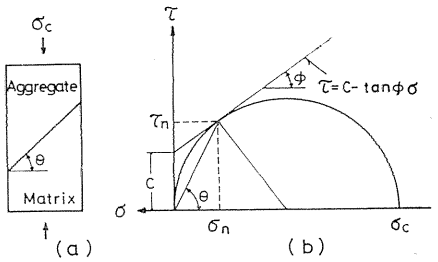

Fig. 2.7. Schematic bond failure criterion at the interface between coarse aggregate and mortar matrix.

2. 3. 2. *Relation between progressive microcracking and particular shape of stress-strain curve of concrete*

In this clause, the progressive microcracking obtained by Exp.-Ⅱ. 2 will be discussed in terms of the particular shape of stress-strain curve of concrete.

Table 2. 5 indicates the stresses at the beginning of propagation of bond crack (σ_b), mortar crack (σ_{mt}), aggregate crack (σ_{at}) and continuous crack (σ_{bm}), together with the compressive strength of plate specimens (F_{cs}). Each of values in Table 2.

Table 2. 5. Stresses at the initiation and propagation of various microcracks.

Notation of specimen	W/C	σ_b (kg/cm²)	σ_{mt} (kg/cm²)	σ_{at} (kg/cm²)	σ_{bm} (kg/cm²)	F_{cs} (kg/cm²)	σ_b/F_{cs}	σ_{mt}/F_{cs}	σ_{at}/F_{cs}	σ_{bm}/F_{cs}
SC-NA	0.45	195	255	—	332	342	0.57	0.75	—	0.97
SC-NA	0.55	156	287	—	260	271	0.58	0.69	—	0.96
SC-NA	0.70	107	122	—	165	172	0.62	0.71	—	0.96
SC-LC	0.55	—	107	135	182	190	—	0.56	0.71	0.96

[Notation] σ_b : Stress at the propagation of bond crack,
σ_{mt} : Stress at the initiation of mortar crack,
σ_{at} : Stress at the initiation of aggregate crack,
σ_{bm} : Stress at the formation of continuous crack interconnected mortar crack to bond crack or aggregate crack,
F_{cs} : Compressive strength of sliced plate specimen.

5 is the average obtained by three specimens. The strains (ε) at the various locations in the specimen are plotted in Figs. 2. 8. 1 through 2. 8. 4 against the stress (σ), together with the stress (σ) - strain (ε) curve of the companion cylinder.

(1) Initial loading stage

The value of strain varies noticeably with the location in the specimen even at the initial loading stage, as shown in Figs. 2. 8. 1 through 2. 8. 4. For normal concrete, the strain of Gage No. 5, i. e., the strain in y-direction at the interface between mortar matrix and the bottom surface of coarse aggregate particle is largest at this loading stage and the rate of increase of strain at this location decreases with stress. However, the strain of Gage No. 6, i. e., the strain in y-direction at the interface between mortar matrix and the top surface of coarse aggregate particle is smaller than that of Gage No. 5 for the same stress level. Accordingly, the large strain of Gage No. 5 was appeared to be resulted from the deformation of weak layer beneath the coarse aggregate particle or potential bond cracks.

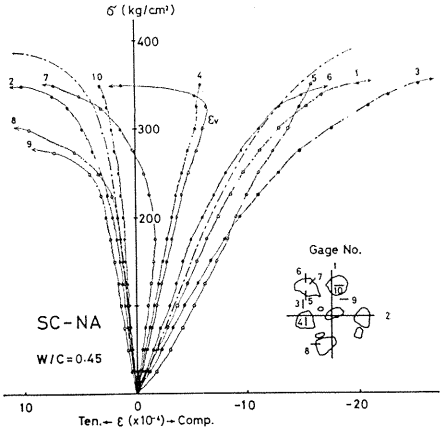

Fig. 2. 8. 1. Normal concrete ($W/C=0.45$)

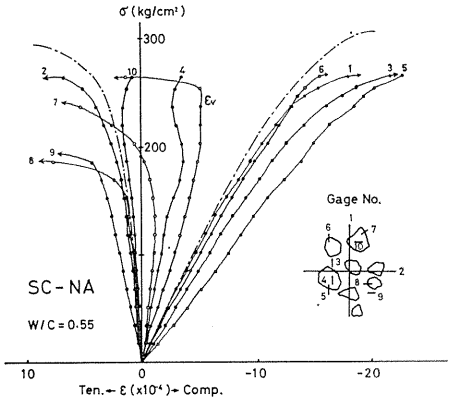

Fig. 2. 8. 2. Normal concrete ($W/C=0.55$)

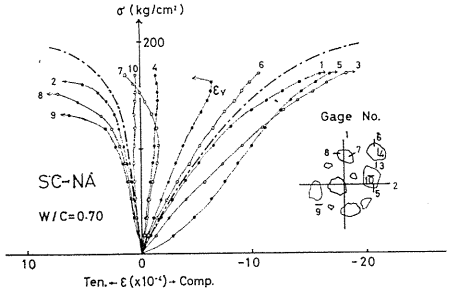

Fig. 2. 8. 3. Normal concrete ($W/C=0.70$)

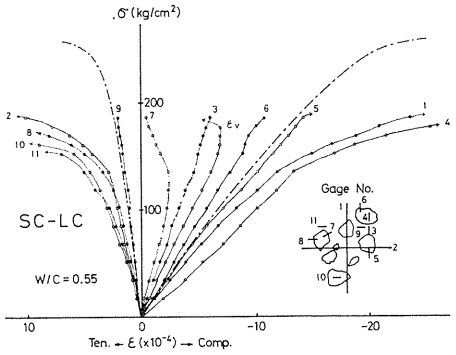

Fig. 2. 8. 4. Lightweight aggregate concrete ($W/C=0.55$)

Fig. 2. 8. Stress (σ) - strain (ε) relation of plate specimen in Exp.- Ⅱ. 2.

The strains of Gage No. 5 at the stress level of 100 kg/cm^2 were approximately 5.2×10^{-4}, 7.3×10^{-4} and 9.3×10^{-4} for normal concretes with $W/C=0.45$, 0.55 and 0.70, and 7.1×10^{-4} for lightweight aggregate concrete with $W/C=0.55$, respectively. Namely, they increase with the increasing water-cement ratio. As shown in Fig. 2. 3, the width of potential bond cracks similarly increased with water-cement ratio. Therefore, it is acceptable that the strain of Gage No. 5 is closely associated with the width of potential bond cracks.

The strain distributions (ε) in y-direction for normal concrete and lightweight aggregate concrete with $W/C=0.55$ are given in Fig. 2. 9, along with the average strain of Gage No. 1. For normal concrete shown in Fig. 2. 9, the strain of Gage No. 3, i. e., the strain of mortar matrix between two coarse aggregate particles is larger than the average strain. Therefore, the stress concentration is induced at this location. For lightweight aggregate concrete, however, the strain of Gage No. 3 is smaller than the average strain. It was examined theoretically by authors[57] that the strain of matrix between two inclusions is smaller than the average, when the elastic modulus of inclusion is smaller than that of matrix. It is considered by the above discussion that the elastic modulus of lightweight aggregate used in Exp.-Ⅱ.2 is smaller than that of mortar matrix. Because all lightweight aggregate particles were cut and their hard shell near the surface was weakened.

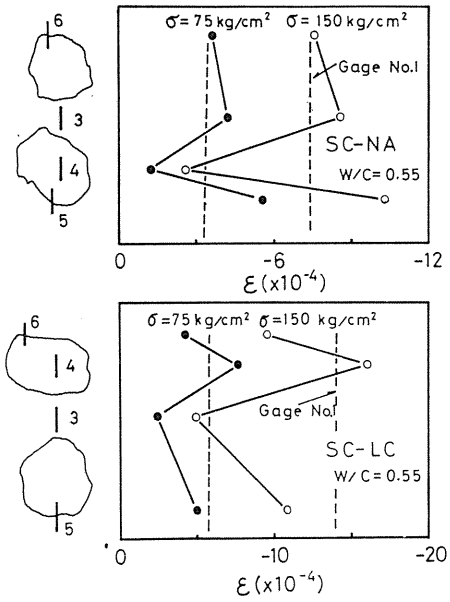

Fig. 2. 9. Strain distribution of plate specimen in longitudinal direction.

(2) Propagation of bond crack

When new bond cracks initiate at the interface between coarse aggregate and mortar matrix, the strains of Gage No. 7 and Gage No. 8 at the interface indicate a particular change. That is, the strain of Gage No. 7 begins to increase rather than decrease with the increasing stress. The relation between the stress and the average strains of Gage No. 1 and Gage No. 2 deviates from linearity.

(3) Occurrence of mortar crack and aggregate crack

For normal concrete at the relative stress level of about 0.7, mortar cracks occur and the rate of increase of strain of Gage No. 9, i. e., the strain of mortar matrix in x-direction adjacent to coarse aggregate becomes larger rapidly. The strain of Gage No. 7 at the interface varies from negative to positive in a few concretes.

For lightweight aggregate concrete, on the other hand, mortar cracks and aggregate cracks occur at the locations of Gage No. 10 and Gage No. 11, respectively, when the stress level is nearly equal to 53 percent of ultimate. The occurrence of these cracks is ahead of propagation of bond crack. This result differs from that obtained by ϕ 10×20 cm cylinders in Exp.-Ⅱ. 1. This difference is probably resulted from that the elastic modulus and strength of sliced lightweight coarse aggregate used in Exp.-Ⅱ. 2 were considerably smaller than those of non-sliced one used in Exp.-Ⅱ. 1.

(4) Formation of continuous crack pattern

At the stress level larger than about 95 percent of ultimate, mortar cracks bridge between bond cracks or aggregate cracks to form long continuous crack patterns and the volume of concrete begins to expand rather than continuing to contract. The strains of mortar matrix (Gage No. 9) and at the interface (Gage No. 8) in x-direction also increase rapidly. For normal concrete, the negative strain of mortar matrix in the neighborhood of the top and bottom surface of coarse aggregate particle (Gage No. 3) becomes very large. It was concluded from these results that the local compressive failure in mortar matrix at this location resulted in failure of normal concrete. For lightweight aggregate concrete, on the other hand, it was estimated that the compressive failure in coarse aggregate led the specimen to failure.

2. 3. 3. Relation between progressive microcracking and characteristic stresses on stress-strain curve of concrete

Several investigators[30)31)34)] have already pointed out that the stress-strain curve of concrete is usually characterized by some critical points, such as proportional limit, initiation stress and critical stress (which are termed "characteristic stresses" in the present paper), and that these points are more or less associated with the progressive microcracking of concrete. If the fracture process of concrete can be indirectly estimated by using such characteristic stresses, the time and effort required for observation of microcracks in concrete will be considerably saved. For such a point of view, the relation between the internal microcracking observed by the direct method and the characteristic stresses on the stress-strain curve obtained by the indirect method is briefly examined here.

Figs. 2. 10. 1 and 2. 10. 2 indicate the relations between σ/F_{cc} and ε, and between σ/F_{cc} and ν_c obtained by Exp.-Ⅱ. 1, where, ε_x and ε_y are longitudinal and circumferential strains measured by 67 mm wire strain gages, respectively, and ε_v is volumetric strain and ν_c is Poisson's ratio calculated by using ε_x and ε_y. The notations of σ_p, σ_{in} and σ_{cr} in Figs. 2. 10. 1 and 2. 10. 2 represent the characteristic stresses generally termed as follows:

σ_p: proportional limit (the stress at which stress-strain curve deviates from linearity)[31)]

σ_{in}: initiation stress (the stress at which Poisson's ratio begins to increase rapidly)[34)]

σ_{cr}: critical stress (the stress at which the volume of concrete begins to expand)[30]

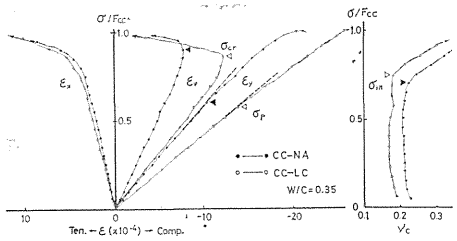

Fig. 2. 10. 1. In the case of $W/C=0.35$

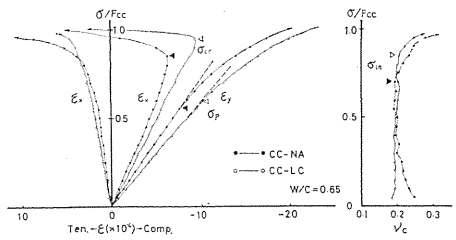

Fig. 2. 10. 2. In the case of $W/C=0.65$

Fig. 2.10. Relation between relative amount of stress (σ/F_{cc}) and various strains (ε).

It is not easy to obtain the above characteristic stresses on the stress-strain curve of concrete and several methods were devised to obtain them. These methods will be discussed in detail in the next chapter.

The test results obtained in the present chapter for the relation between the progressive microcracking and the characteristic stresses are summarized as follows:

i) The ratio of the proportional limit to the compressive strength (σ_p/F_{cc}) was about 0.55-0.60, independently of the type of coarse aggregate and the strength of mortar matrix, and the proportional limit was in good agreement with the stress at which bond cracks began to propagate at the interface between coarse aggregate and mortar matrix. Therefore, the proportional limit is likely to correspond to the first change of the macroscopic surface strain due to the microscopic structural change in concrete.

ii) The ratio of the initiation stress to the compressive strength (σ_{in}/F_{cc}) was about 0.7-0.75 for lightweight aggregate concrete with $W/C=0.35$ and for normal concrete, and about 0.85 for lightweight aggregate concrete with $W/C=0.65$. The initiation stress correlated well with the stress at which mortar cracks or aggregate cracks occurred.

iii) The ratio of the critical stress to the compressive strength (σ_{cr}/F_{cc}) was about 0.85-0.9 for lightweight aggregate concrete with $W/C=0.35$ and for normal concrete, and about 0.95 for lightweight aggregate with $W/C=0.65$. The critical stress was in good agreement with the stress at which the mortar cracks bridged between bond cracks or aggregate cracks to form continuous crack patterns.

As described above, the characteristic stresses are closely related to the internal microcracking in concrete. Therefore, it will be possible to estimate the fracture process of concrete by such a simple and convenient indirect method.

2. 4. Conclusion

In this chapter, the progressive microcracking in concrete was examined with a microscope and was related to the particular shape of stress-strain curve of concrete made with artificial lightweight aggregate and river gravel.

The test results obtained in the present chapter are summarized as follows:

1) The progressive microcracking in concrete varies considerably with the type of coarse aggregate used and the strength of mortar matrix. The fracture

process of concrete is generally characterized by the initiation and propagation of bond cracks, mortar cracks and aggregate cracks, the formation of continuous crack patterns consisting of these cracks, and the local compressive failure in mortar matrix or coarse aggregate.

2) The potential bond cracks are present beneath the coarse aggregate particles even before loading and their maximum width increases with the increase of water-cement ratio of mortar matrix.

3) Bond cracks between coarse aggregate and mortar matrix cause the first structural change of concrete, regardless of the type of coarse aggregate and the strength of mortar matrix.

4) For normal concrete, the order of microcracking or fracture process was as follows: (1) beginning of bond crack, (2) appearance of longitudinal tensile cracking in mortar matrix, and (3) local compressive failure in mortar matrix at the vicinity of coarse aggregate.

5) The order of fracture process of lightweight aggregate concrete varies with the strength of mortar matrix. The order of fracture process of low compressive strength concrete with high water-cement ratio was the same to that of normal concrete, but the fracture process of high compressive strength concrete was as follows: (1) beginning of bond crack, (2) simultaneous appearance and growth of tensile crack in mortar matrix and in coarse aggregate, and (3) compressive failure in coarse aggregate.

6) Proportional limit, initation stress and critical stress on the stress-strain curve of concrete correlate well with the stresses at which bond cracks begin to propagate, mortar cracks initiate and continuous cracks are formed, respectively. Therefore, the fracture process of concrete can be indirectly estimated by the measurement of these characteristic stresses.

3. Characteristic Stresses on Stress-Strain Curve of Concrete

3. 1. Introduction

It was clarified in Chapter 2 that the characteristic stresses such as proportional limit, initiation stress and critical stress on the stress-strain curve of concrete, are closely related to the progressive microcracking in concrete, and that the fracture process of concrete can be indirectly estimated by the method utilizing these characteristic stresses.

The object of the present chapter is to examine, by the indirect method, the effect of variables related to aggregate, such as the type, size, volume fractions of fine and coarse aggregates, and the effect of variables related to cement paste or mortar matrix, such as water-cement ratio and volume fraction of cement on the fracture process of concrete.

Many investigators[30)~42)] have already studied on the characteristic stresses of concrete. The summary of previous investigations is indicated in Table 3. 1, together with the kind, the observation methods and the observed values of characteristic stresses.

Let us discuss briefly on each of characteristic stresses obtained by previous studies.

Table 3. 1. Previous studies on characteristic stresses on stress-strain curve of concrete.

Classification	Investigators	Method of determination	Relative characteristic stresses σ/F_{cc}	Variation of σ/F_{cc}
Proportional limit	Kaplan[31]	Proportional limit of $\sigma-\varepsilon_y$ curve	0.46-0.51	slight change by varying W/C
	Yokomichi・Kakuta・Ayuta[35]	First kink on $\log\sigma-\log\varepsilon_y$	0.5 -0.6	decrease with increasing V_{ca}/V_{cc}
	Okamoto・Yamamoto[37]	Proportional limit of $\sigma-\varepsilon_y$ curve	0.4 -0.5	independent of F_{cc}
	Kato[27]	Proportional limit of $\sigma-\varepsilon_y$ curve	0.51-0.64	increase with increasing F_{cc}
	Hasaba・Kawamura[38]	First change of ν_c	0.40-0.55	increase with increasing F_{cc}
	Hasaba・Kawamura[38]	First change of $\Delta\varepsilon_x/\Delta\sigma$	0.45-0.60	and decreasing V_{ca}/V_{cc}
	Okushima・Suzuki・Nakatsuka[41]	First kink on $\log\sigma-\log\varepsilon_y$	0.5 -0.7	slight decrease with increasing F_{cc}
Initiation stress	Béres[33]	First kink on $\sigma-\nu_c$ curve	0.47-0.85	increase with increasing age
	Shah・Chandra[34]	First kink on $\sigma-\nu_c$ curve	0.45-1.00	decrease with increasing V_{ca}/V_{cc}
	Okamoto・Yamamoto[37]	First kink on $\sigma-\nu_c$ curve	0.75-1.00	decrease with increasing V_{ca}/V_{cc}
	Yokomichi・Kakuta・Ayuta[35]	First kink on $\sigma-\nu_c$ curve	0.9 -0.95	decrease with increasing V_{ca}/V_{cc}
	Kato[27]	First kink on $\sigma-\nu_c$ curve	0.69-0.88	increase with increasing F_{cc}
	Hasaba・Kawamura[38]	First kink on $\sigma-\nu_c$ curve	0.7 -0.8	slight increase with increasing F_{cc}
	Okushima・Suzuki・Nakatsuka[41]	First kink on $\sigma-\nu_c$ curve	0.5 -0.95	decrease with increasing F_{cc}
Critical stress	Brandtzaeg[30]	Beginning of increase of ε_v	0.77-0.85	
	Shah・Chandra[34]	Beginning of increase of ε_v	0.81-1.00	decrease with increasing size of aggregate
	Okamoto・Yamamoto[37]	Beginning of increase of ε_v	0.8 -1.0	decrease with increasing V_{ca}/V_{cc}
	Kato[27]	Beginning of increase of ε_v	0.70-0.95	increase with increasing F_{cc}
	Hasaba・Kawamura[38]	Beginning of increase of ε_v	0.6 -0.8	increase with increasing V_{ca}/V_{cc}
	Okushima・Suzuki・Nakatsuka[41]	Beginning of increase of ε_v	0.8 -1.0	independent of F_{cc}

[Notation] σ: Stress, ε_y: Longitudinal strain, ε_x: Circumferential strain, ε_v: Volumetric strain, ν_c: Poisson's ratio, V_{ca}/V_{cc}: Volume fraction of coarse aggregate, F_{cc}: Compressive strength.

1) Proportional limit; Proportional limit of concrete (σ_p) was defined by Kaplan[31] as the stress at which the longitudinal strain subtracted by the strain which is calculated by using "the trial modulus of elasticity" of concrete becomes larger than 2×10^{-6}. Kaplan has pointed out that the ratio of the proportional limit to the compressive strength of concrete (σ_p/F_{cc}) is about 0.46-0.51, regardless of the water-cement ratio. On the other hand, Kato[27] has reported that the relative proportional limit (σ_p/F_{cc}) obtained by a similar method as Kaplan's increases with the strength of concrete.

Some investigators[32)35)40)] have ascertained that the stress-strain curve of concrete illustrated in a logarithmic graph is generally represented by three straight lines, namely, two kinks are present on log stress-log strain plots of concrete. It may be considered that the first kink corresponds to the proportional limit. Yokomichi, Kakuta and Ayuta[35] have found that the ratio of the proportional limit obtained by this method to the compressive strength is hardly influenced by the water-cement ratio, but Okushima et al.[41] have reported that this ratio decreases with the increasing strength of concrete.

2) Initiation stress; Initiation stress of concrete (σ_{in}) is generally defined as the stress at which Poisson's ratio of concrete begins to increase continuously. Shah and Chandra[34] have found that the initiation stress represents the beginning of significant inelastic behavior of concrete. There have already been several studies on the initiation stress of concrete. However, the conclusions obtained by these studies are not necessarily consistent and the following two opposite results have been reported: the one[27] that the relative initiation stress (σ_{in}/F_{cc}) increases with the compressive strength of concrete (F_{cc}) and the other[41] that the value of σ_{in}/F_{cc} decreases with the value of F_{cc}.

3) Critical stress; Critical stress of concrete (σ_{cr}) was first recognized by Brandtzaeg[30]. At the stress level equal to the critical stress, the volume of concrete begins to increase rather than continue to decrease. Since the critical stress correlates well with the ultimate strength of concrete under repeated and long time sustained loading, this stress has been often called "true ultimate strength" or "real strength"[32]. Many investigators have studied on the critical stress of concrete but the various conclusions were obtained. For example, Kato [27], Béres[33] and Hasaba et al.[38] have reported respectively that the relative critical stress (σ_{cr}/F_{cc}) increases, decreases and does not vary with the strength of concrete.

As described above, many investigators have examined the characteristic stresses on the stress-strain curve of concrete but the results obtained are very conflicting. This fact is probably resulted from that the method of testing and the materials used varied with each of investigations and the substantially identical phenomenon was understood from different standpoints.

Therefore, the following comprehensive investigations were programmed in the present chapter for the examination of the effect of variables related to coarse aggregate and mortar matrix on the characteristic stresses of concrete, including cement paste or mortar matrix.

3. 2. Test procedure

3. 2. 1. Outline of experiments

The following four series and eight kinds of experiment were carried out by using ϕ 10×20 cm cylindrical specimens.

1) Experiment-Ⅲ. 1; The experiment for cement paste with various water-cement ratio (W/C). (hereafter called "P-series").

2) Experiment-Ⅲ. 2; The experiment for mortar matrix with various types and volume fractions of fine aggregate in mortar (V_{sa}/V_m). ("M-series").

i) Exp.-Ⅲ. 2. 1: The one for the examination of the effect of type and volume fraction of fine aggregate.

ii) Exp.-Ⅲ. 2. 2: The one for the examination of the effect of water-cement ratio.

3) Experiment-Ⅲ. 3; The experiment for concrete consisting of cement paste matrix and coarse aggregate with various types, sizes (ϕ_a) and volume fractions in concrete (V_{ca}/V_{cc}). ("PC-series").

4) Experiment-Ⅲ. 4; The experiment for concrete cosisting of mortar matrix and coarse aggregate with various types, sizes (ϕ_a) and volume fractions in concrete (V_{ca}/V_{cc}). ("MC-series").

i) Exp.-Ⅲ. 4. 1: The one in which the effect of type and size of coarse aggregate and water-cement ratio of mortar matrix is mainly examined. In this experiment, the effect of restraint from friction at the ends of specimen on the critical stress is also examined.

ii) Exp.-Ⅲ. 4. 2: The one in which the effect of type and volume fraction of coarse aggregate is mainly examined.

iii) Exp.-Ⅲ. 4. 3: The one in which the effect of water-cement ratio of mortar matrix is mainly examined by using the concrete specimens with a constant volume fraction of fine and coarse aggregate.

iv) Exp.-Ⅲ. 4. 4: The one in which the effect of water-cement ratio of mortar matrix is mainly examined by using concrete specimens with some of mix proportions described in JASS 5.

Outline of the experiments is shown in Table 3. 2.

Table 3. 2. Outline of experiments.

Table 3. 2. 1. Experiment-Ⅲ. 1.

Cement used	W/C
Ordinary Portland cement	0.25, 0.30, 0.35, 0.40 0.45, 0.50, 0.55, 0.60

Table 3. 2. 2. Experiment-Ⅲ. 2.

Notation of experiment	Notation of specimen	Type of fine aggregate	W/C	V_{sa}/V_m
Exp.-Ⅲ. 2. 1	M-NA	River sand	0.4	0.0, 0.1, 0.2, 0.3, 0.4, 0.5, 0.6, 0.7
	M-LP	Lightweight aggregate (LP)		
	M-LC	〃 (LC)		
Exp.-Ⅲ. 2. 2.	M-NA	River sand	0.35, 0.40, 0.45 0.55, 0.65	0.4
	M-LC	Lightweight aggregate (LC)		

[Notation] LP: Pelletized-type lightweight aggregate,
LC: Coated-type lightweight aggregate.

Table 3. 2. 3. Experiment-Ⅲ. 3.

Notation of specimen	Type of coarse aggregate	ϕ_a (mm)	W/C	V_{ca}/V_{cc}
PC-NA	River gravel	15-20	0.40	0, 0.3, 0.4, 0.5, 0.6, 0.7
PC-LP	Lightweight aggregate (LP)	15-20	0.40	
PC-LC	Lightweight aggregate (LC)	15-20	0.40	
PC-DA	Crushed andesite	10-15, 15-20, 20-25	0.40	
PC-SA	Crushed sandstone	10-15, 15-20, 20-25	0.40	
PC-LI	Crushed limestone	15-20	0.40	
PC-G	Glass beads	13, 18, 28	0.30	
PC-S	Steel ball	18	0.30	

[Notation] ϕ_a: Size range of coarse aggregate, W/C: Water-cement ratio by weight, V_{ca}/V_{cc}: Volume fraction of coarse aggregate,
LP: Pelletized-type lightweight aggregate,
LC: Coated-type lightweight aggregate.

Table 3. 2. 4. Experiment-Ⅲ. 4.

Notation of experiment	Notation of specimen	Type of aggregate: Fine	Type of aggregate: Coarse	ϕ_a (mm)	W/C	V_{ca}/V_{cc}	V_{sa}/V_a
Exp.-Ⅲ. 4.1	MC-NA	River sand	River gravel	20-25	0.55	0.3	0.52
				10-15	0.45	0.3	0.52
				10-15	0.55	0.15, 0.3, 0.4	0.73, 0.52, 0.60
				10-15	0.70	0.3	0.52
				2.5-5	0.55	0.3	0.52
	MC-LC	River sand	Lightweight aggregate (LC)	10-15	0.45	0.3	0.52
				10-15	0.55	0.15, 0.3, 0.4	0.73, 0.52, 0.60
				10-15	0.70	0.3	0.52
Exp.-Ⅲ. 4.2	MC-NA	River sand	River gravel	15-20	0.40	0, 0.15, 0.20, 0.25, 0.3, 0.35	0.5
	MC-LP	River sand	Lightweight agg. (LP)	15-20	0.40		
	MC-LC	River sand	Lightweight agg. (LC)	15-20	0.40		
Exp.-Ⅲ. 4.3	MC-NA	River sand	River gravel	10-15	0.35, 0.40	0.3	0.48
	MC-LC		Lightweight aggregate (LC)	10-15	0.45, 0.55, 0.60		
Exp.-Ⅲ. 4.4	MC-NA	River sand	River gravel	10-15	0.45	0.39	0.41
					0.50	0.39	0.43
					0.55	0.39	0.44
					0.60	0.39	0.45
					0.65	0.39	0.47
					0.70	0.36	0.48

[Notation] ϕ_a: Size range of coarse aggregate, W/C: Water-cement ratio,
V_{ca}/V_{cc}: Volume fraction of coarse aggregate,
V_{sa}/V_a: Ratio of fine aggregate to total aggregate by volume,
V_a: Volume of total aggregate in concrete.

3. 2. 2. Fabrication and curing of specimen

(1) Materials used

1) Cement; Ordinary Portland cement was used in all experiments. The compressive strength of cement used was 410-418 kg/cm^2 at the age of 28 days.

2) Fine aggregate; Kiso-river and Machiya-river sands, and coated and pelletized type lightweight aggregates (maximum size=5 mm) were used for fine aggregate.

3) Coarse aggregate; Kiso-river gravel, coated and pelletized type lightweight aggregates, crushed andesite, limestone and sandstone, glass beads and steel ball were used for coarse aggregate. The properties of aggregate used are shown in Table 3. 3.

Table 3. 3. Properties of aggregates used.

Notation of experiment	Type		Size range (mm)	Specific gravity	Fineness modulus	Bulk density (kg/m^3)	Water absorption (%)	10% crushing value (ton)
Exp.-Ⅲ. 2 Exp.-Ⅲ. 3 Exp.-Ⅲ. 4.2 Exp.-Ⅲ. 4.3	River sand and gravel	Fine	0-5	2.61	3.82	1692	1.54	—
		Coarse	15-20	2.52	7.00	1570	0.82	23.7
	Lightweight aggregate (pelletized-type)	Fine	0-5	1.94	3.63	1354	8.70	—
		Coarse	15-20	1.30	7.00	867	2.78	10.8
	Lightweight aggregate (coated-type)	Fine	0-5	1.40	4.01	1254	16.72	—
		Coarse	15-20	1.35	7.00	843	11.85	8.9
Exp.-Ⅲ. 3	Crushed sandstone	Small	10-15	2.88	6.18	1570	0.67	21.4
		Middle	15-20	2.79	7.02	1560	0.81	—
		Large	20-25	2.67	7.67	1574	0.82	—
	Crushed andesite	Small	10-15	2.70	6.25	1595	0.40	25.8
		Middle	15-20	2.72	7.06	1574	0.55	—
		Large	20-25	2.67	7.68	1595	0.32	—
	Crushed limestone	—	15-20	2.91	7.25	1673	0.39	19.2
	Glass beads	—	13, 18, 28	2.25	—	—	—	—
	Steel ball	—	18	7.80	—	—	—	—
Exp.-Ⅲ. 4.1	River sand	—	0-2.5	2.59	1.99	1720	2.10	—
	River gravel	Small	2.5-5	2.57	5.00	1675	0.98	—
		Middle	10-15	2.55	7.00	1642	0.57	—
		Large	20-25	2.52	8.00	1600	0.58	—
	Lightweight aggregate (coated-type)	—	10-15	1.32	7.00	798	8.16	—
Exp.-Ⅲ. 4.4	River sand and gravel	Fine	0-5	2.59	3.24	1670	2.62	—
		Coarse	5-20	2.58	6.71	1661	1.54	—
	Lightweight aggregate (coated-type)	—	5-20	1.35	6.42	849	8.76	—

The compressive strength (F_{ca}), modulus of elasticity (E_a) and Poisson's ratio (ν_a) of Kiso-river gravel, crushed limestone and sandstone were measured by using 4×4×8 cm prismatic specimens made by cutting from large boulders taken from the same location as these aggregates. The measured values are shown in Table 3. 4.

Table 3. 4. Mechanical properties of aggregate.

Type of aggregate	Compressive strength F_{ca} (kg/cm²)	Modulus of elasticity E_a (kg/cm²)	Poisson's ratio ν_a
River gravel	670	6.57×10^5	0.17
Sandstone	693	6.24×10^5	0.19
Limestone	580	5.72×10^5	0.23

(2) Outline of mix proportions

Outline of mix proportions has already shown in Tables 3. 2. 1 through 3. 2. 4. For concretes in Exp.-Ⅲ. 4. 1, the volume fraction of fine aggregate in total aggregate (V_{sa}/V_a) was varied with the volume fraction of coarse aggregate in concrete so as to obtain a workable mix, whereas for concretes in Exp.-Ⅲ. 4. 2, the value of V_{sa}/V_a was kept to a constant value so as to examine the effect of the volume fraction of total aggregate on the characteristic stresses of concrete. On the other hand, for concretes in Exp.-Ⅲ. 4. 4, the volume fractions of fine and coarse aggregates varied with the water-cement ratio, since the mix proportions were determined in accordance with the recommended values in JASS 5.

(3) Fabrication and curing of specimen

ϕ 10×20 cm cylindrical specimens were cast in steel molds and compacted by a vibrating rod. The specimens were stored in the laboratory during about 48 hours after casting, then remolded and cured in water of a temperature of 20°±1°C up to the day before testing. All tests were carried out at the age of 28 days.

3. 2. 3. Methods of loading and measurement

With a few exceptions, the specimens were loaded in accordance with the specified method in JIS A 1108. The loading rate was kept to about 2-3 kg/cm²/sec. Several specimens in Exp.-Ⅲ. 4. 1, the lubricating pads consisting of a rubber sheet (0. 3 mm in thickness) and an aluminium film (0. 1 mm in thickness) with lubricated surface by silicon grease were inserted between the ends of specimen and the loading platens, to minimize the frictional restraint effect of lateral deformation of concrete. The coefficient of friction between the ends of specimen and the loading platens in this case was about 0. 005.

The longitudinal strain (ε_y) and the circumferential strain (ε_x) were measured by 67 mm wire strain gages and the volumetric strain ($\varepsilon_v=\varepsilon_y-2\varepsilon_x$) and Poisson's ratio ($\nu_c=\varepsilon_x/\varepsilon_y$) were calculated by using the measured values of ε_x and ε_y. A digital strain meter was applied for the strain measurements.

3. 3. Test results and discussion

3. 3. 1. Method of determination of characteristic stresses

The previous methods for determining the characteristic stresses have been already outlined in Table 3. 1. Among them, the method for determining the critical stress by using the stress (σ)-volumetric strain (ε_v) curve is convenient and the personal factor is hardly involved in judging the value. However, several methods in Table 3. 1 are not necessarily applicable for the practical use, since the characteristic stresses cannot be easily obtained and the personal factor is involved in determining their values. Especially for the determination of initiation stress, different methods from that suggested by Shah and Chandra[34] will be required. Therefore, several methods applicable to the determination of characteristic stresses of concrete will be briefly discussed in this clause.

Fig. 3. 1 shows a typical example of the relation between the circumferential strain (ε_x) and the longitudinal strain (ε_y) obtained by Exp.-Ⅲ. 4. 3. The relation can be generally represented by four straight lines. It is comparatively easy to obtain three kinks determined by four straight lines. Let us designate these three kinks as σ_{a1}, σ_{a2} and σ_{a3} (points A, B and C in Fig. 3. 1, respectively) in the smaller order of strain.

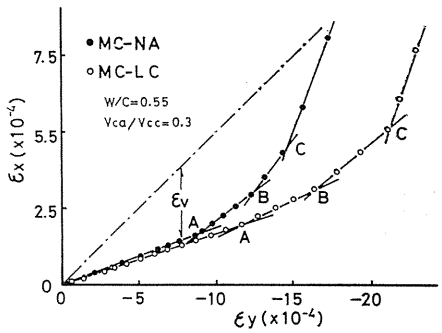

Fig. 3. 1. Relation between circumferential strain (ε_x) and longitudinal strain (ε_y).

On the other hand, Fig. 3. 2 shows a typical example of the relation between the stress (σ) and the longitudinal strain (ε_y) illustrated in a logarithmic graph. The relation can be usually represented by three straight lines, as ascertained by Desayi[32] and Yokomichi et al.[35] Let us designate two kinks formed by these straight lines as σ_{l1} and σ_{l2} in the smaller order of stress. Determination of the values of σ_{l1} and σ_{l2} is easier than that of the values of σ_{a1}, σ_{a2} and σ_{a3} described above.

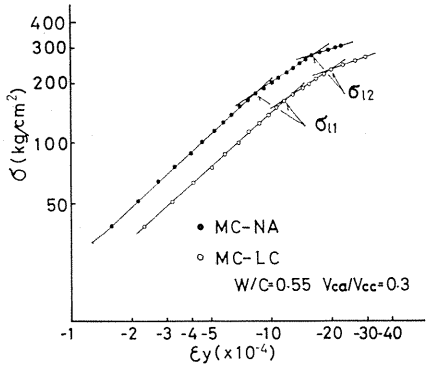

Fig. 3. 2. Relation between log σ and log ε_y.

Next, let us consider how these kinks relate to proportional limit (σ_p), initiation stress (σ_{in}) or critical stress (σ_{cr}). Table 3. 5 indicates the ratios of observed values of σ_p, σ_{in}, σ_{cr}, σ_{a1}, σ_{a2}, σ_{a3}, σ_{l1} and σ_{l2} to the compressive strength (F_{cc}) for normal concrete (MC-NA) and lightweight aggregate concrete (MC-LC) with $W/C=0.55$ in Exp.-Ⅲ. 4. 3. As shown in Table 3. 5, the observed values of σ_{a1} and σ_{l1} are in good agreement with proportional limit (σ_p), and the values of σ_{a3} and σ_{l2} with critical stress (σ_{cr}). Whereas, the

value of σ_{a2} approximately coincides with initiation stress (σ_{in}).

Table 3. 5. Characteristic stresses obtained by various methods.

Type of concrete	σ_p/F_{cc}	σ_{a1}/F_{cc}	σ_{l1}/F_{cc}	σ_{in}/F_{cc}	σ_{a2}/F_{cc}	σ_{cr}/F_{cc}	σ_{a3}/F_{cc}	σ_{l2}/F_{cc}
MC-NA	0.58	0.58	0.57	0.75	0.78	0.84	0.86	0.86
MC-LC	0.64	0.65	0.65	0.84	0.82	0.94	0.96	0.96

Consequently, in the present paper, the characteristic stresses on the stress-strain curve of concrete were determined by using ε_x-ε_y curve, $\log\sigma$-$\log\varepsilon_y$ curve and σ-ε_v curve, in which the characteristic stresses can be determined without difficulty and personal factor.

3. 3. 2. Characteristic stresses of cement paste

(1) Properties of characteristic stresses

The relation between σ_p/F_{cp}, σ_{in}/F_{cp} and σ_{cr}/F_{cp} and W/C obtained by Exp.-Ⅲ. 1 for cement paste is indicated in Fig. 3. 3, where, F_{cp} is the compressive strength of cement paste. As in Fig. 3. 3, the relative proportional limit (σ_p/F_{cp}) of cement paste increases slightly as the water-cement ratio is increased. The proportional limit of concrete was approximately consistent with the stress at which the bond cracks at the interface between coarse aggregate and mortar matrix begin to propagate, as described in Chapter 2. The proportional limit was observed even in cement paste which has no aggregate. This is probably resulted from that cement paste is considered as one kind of composite material consisting of cement gel and unhydrated cement particles and microcracks occur at the vicinity of unhydrated cement particles or air voids prior to failure of specimen.

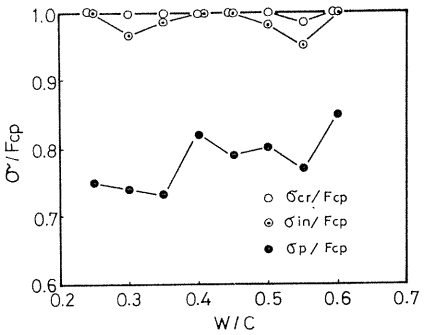

Fig. 3. 3. Relation between relative characteristic stresses (σ/F_{cp}) and water-cement ratio (W/C) of cement paste.

The relative proportional limit (σ_p/F_{cp}) is plotted in Fig. 3. 4 against the volume fraction of cement particles in cement paste (V_c/V_{cp}), where, V_c/V_{cp} is related to W/C by the following equation.

$$V_c/V_{cp}=\frac{1}{\rho_c(W/C)+1} \tag{3. 1}$$

where, ρ_c : specific gravity of cement.

The relative proportional limit of cement paste (σ_p/F_{cp}) tends to decrease with the increase of V_c/V_{cp}, as shown in Fig. 3. 4.

On the other hand, the initiation stress (σ_{in}) and the critical stress (σ_{cr}) of cement paste were approximately equal to the compressive strength (F_{cp}). This fact may be resulted from that the cement paste specimen fails immediately after

the propagation of the microcracks parallel to the longitudinal axis, since there is no aggregate as a crack arrestor in cement paste.

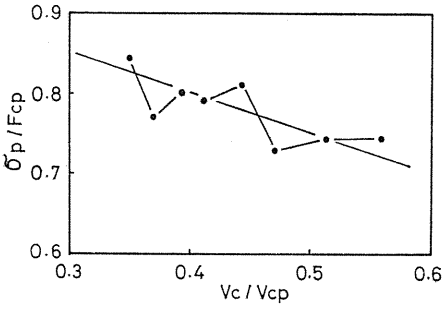

Fig. 3. 4. Relation between relative proportional limit (σ_p/F_{cp}) and volume fraction of cement (V_c/V_{cp}) of cement paste.

(2) Empirical equations for characteristic stresses

The following equations for the characteristic stresses of cement paste were obtained by Exp.-Ⅲ. 1.

$$\sigma_p/F_{cp}=1-0.5(V_c/V_{cp}) \tag{3. 2}$$

$$\sigma_{in}/F_{cp}=1 \tag{3. 3}$$

$$\sigma_{cr}/F_{cp}=1 \tag{3. 4}$$

3. 3. 3. Characteristic stresses of mortar

(1) Properties of characteristic stresses of mortar

The relation between σ_p/F_{cm}, σ_{in}/F_{cm} and σ_{cr}/F_{cm} of mortar made of various fine aggregates, and V_{sa}/V_m obtained by Exp.-Ⅲ. 2. 1 is indicated in Fig. 3. 5, where, F_{cm} and V_{sa}/V_m are the compressive strength of mortar and the volume fraction of fine aggregate, respectively. The relative characteristic stresess (σ_p/F_{cm}, σ_{in}/F_{cm} and σ_{cr}/F_{cm}) decrease as the volume fraction of fine aggregate (V_{sa}/V_m) is increased. This phenomenon may be caused by that the bond cracks are likely to initiate and propagate at the interface between fine aggregate particles and cement paste matrix, because the area of interface increases with the value of V_{sa}/V_m.

The relative initiation stress (σ_{in}/F_{cm}) and the relative critical stress (σ_{cr}/F_{cm}) of mortar are approximately constant, independently of the volume fraction of cement in cement paste (V_c/V_{cp}), as shown in Fig. 3. 6. However, the relative proportional limit (σ_p/F_{cm}) slightly decreases as the volume fraction of cement in cement paste (V_c/V_{cp}) is increased, because the value of σ_p/F_{cp} of cement

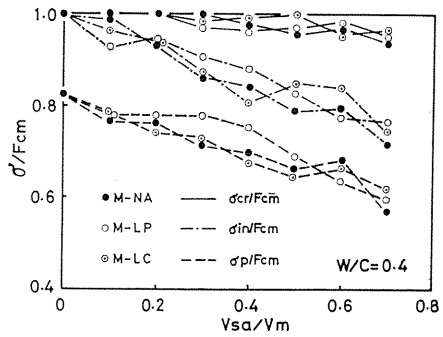

Fig. 3. 5. Relation between relative characteristic stresses (σ/F_{cm}) and volume fraction of fine aggregate (V_{sa}/V_m) of mortar.

paste matrix decreases with the increase of V_c/V_{cp}.

(2) Empirical equations for characteristic stresses

The following empirical equations were obtained by Exp.-Ⅲ. 2.

$$\sigma_p/F_{cm}=1-0.5(V_c/V_{cp})-0.3(V_{sa}/V_m) \tag{3. 5}$$

$$\sigma_{in}/F_{cm}=1-0.35(V_{sa}/V_m) \tag{3. 6}$$

$$\sigma_{cr}/F_{cm}=1-0.05(V_{sa}/V_m) \tag{3. 7}$$

Eqs. (3. 5), (3. 6) and (3. 7) correspond to Eqs. (3. 2), (3. 3) and (3. 4) for cement paste, respectively, when the value of V_{sa}/V_m is zero.

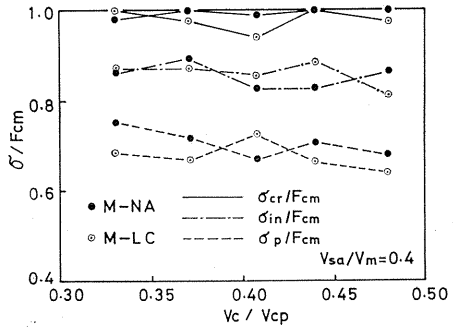

Fig. 3. 6. Relation between relative characteristic stresses (σ/F_{cm}) and volume fraction of cement (V_c/V_{cp}) of mortar.

3. 3. 4. Characteristic stresses of concrete

(1) Properties of characteristic stresses

1) Effect of volume fraction of coarse aggregate

Figs. 3. 7 and 3. 8 show the relation between σ_p/F_{cc}, σ_{in}/F_{cc} and σ_{cr}/F_{cc}, and V_{ca}/V_{cc} obtained by Exp.-Ⅲ. 3 for PC-series concretes consisting of cement paste with $W/C=0.4$ and river gravel (NA), coated type lightweight aggregate (LC) or pelletized type lightweight aggregate (LP), where, F_{cc} and V_{ca}/V_{cc} are the compressive strength of concrete and the volume fraction of coarse aggregate in concrete, respectively. Each of the relative characteristic stresses (σ/F_{cc}) tends to decrease with the increasing volume fraction of coarse aggregate (V_{ca}/V_{cc}). This reason may be considered as follows: As the area of interface between coarse aggregate particle and cement paste and the stress concentration in cement paste or coarse aggregate become larger with the increasing value of V_{ca}/V_{cc}, the various microcracks are likely to initiate and propagate at the smaller stress level.

On the other hand, the proportional limit and the initiation stress of concrete with $W/C=0.4$ as shown in Figs. 3. 7 and 3. 8 are hardly affected by the type of coarse aggregate used, but the critical stress is slightly larger in lightweight aggregate concrete than in normal concrete at the same compressive strength. This fact is probably resulted from that the energy required from the occurrence of continuous cracks up to failure of concrete is larger in normal concrete, since the continuous cracks in normal concrete generally propagate around the coarse aggregate. While, the continuous cracks in lightweight aggregate concrete with $W/C=0.4$ usually penetrated the coarse aggregate, as described in Chapter 2.

Figs. 3. 9 and 3. 10 show the relation between σ_p/F_{cc}, σ_{in}/F_{cc} and σ_{cr}/F_{cc}, and

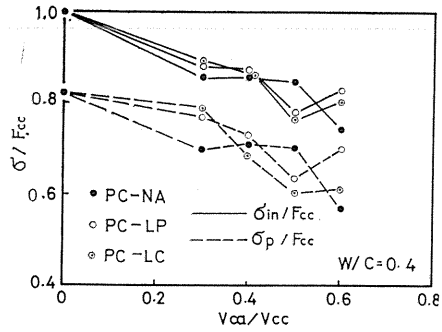

Fig. 3. 7. Relation between relative characteristic stresses (σ/F_{cc}) and volume fraction of coarse aggregate (V_{ca}/V_{cc}) of PC-series concrete.

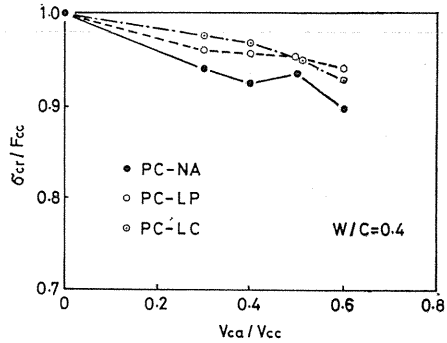

Fig. 3. 8. Relation between relative critical stress (σ_{cr}/F_{cc}) and volume fraction of coarse aggregate (V_{ca}/V_{cc}) of PC-series concrete.

V_{ca}/V_{cc} obtained by Exp.-Ⅲ. 4. 2 for MC-series concrete. The ratios of characteristic stresses to the compressive strength of concrete (σ/F_{cc}) decrease with the increase of volume fraction of coarse aggregate (V_{ca}/V_{cc}). However, the proportional limit and the initiation stress of MC-series concrete are smaller than those of PC-series concrete at a given compressive strength and volume fraction of coarse aggregate. This phenomenon can be explained as follows: The characteristic stresses of PC-series concrete are influenced by only the volume fraction of coarse aggregate, because PC-series concrete was made with cement paste matrix. While, the characteristic stresses of MC-series concrete are influenced by the volume fractions of both fine and coarse aggregates, because the volume fraction of fine aggregate in total aggregate was kept to 0. 5. As described previously, the characteristic stresses of mortar matrix decrease with the increase of volume fraction of fine aggregate in mortar matrix. Accordingly, the characteristic stresses of MC-series concrete become smaller than those of PC-series concrete.

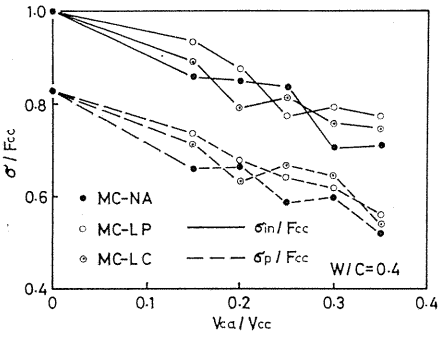

Fig. 3. 9. Relation between relative characteristic stresses (σ/F_{cc}) and volume fraction of coarse aggregate (V_{ca}/V_{cc}) of MC-series concrete.

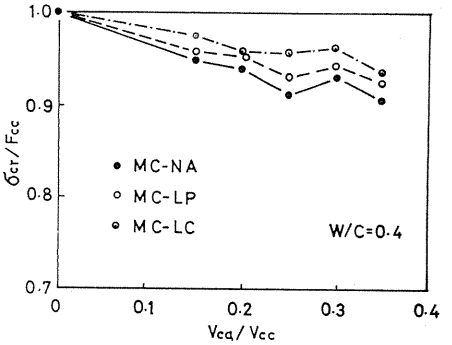

Fig. 3. 10. Relation between relative critical stress (σ_{cr}/F_{cc}) and volume fraction of coarse aggregate (V_{ca}/V_{cc}) of MC-series concrete.

2) Effect of strength of mortar matrix

In this clause, the effect of the strength of mortar matrix on the characteristic

stresses of concrete is examined in terms of the volume fraction of cement in cement paste (V_c/V_{cp}). The value of V_c/V_{cp} is approximately proportional to the compressive strength of concrete, since it is inversely proportional to W/C, as shown by Eq. (3. 1).

Figs. 3. 11 and 3. 12 indicate the relation between the relative characteristic stresses (σ/F_{cc}) and V_c/V_{cp} for MC-series concrete obtained by Exp.-Ⅲ. 4. 3. The results obtained from Figs. 3. 11 and 3. 12 are summarized as follows:

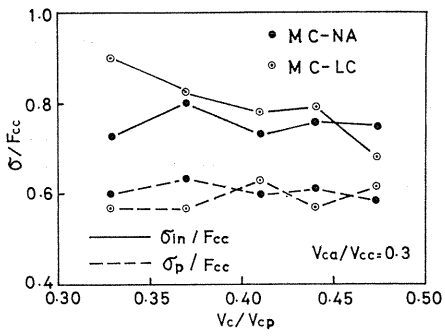

Fig. 3. 11. Relation between relative characteristic stresses (σ/F_{cc}) and volume fraction of cement (V_c/V_{cp}) of MC-series concrete.

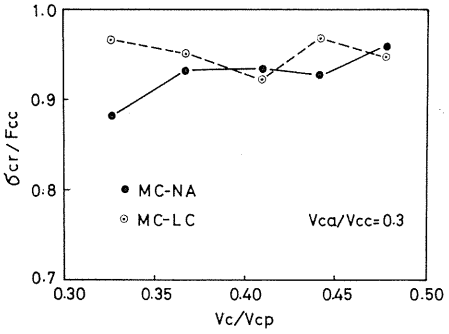

Fig. 3. 12. Relation between relative critical stress (σ_{cr}/F_{cc}) and volume fraction of cement (V_c/V_{cp}) of MC-series concrete.

i) Relative proportional limit (σ_p/F_{cc}) is hardly influenced by the volume fraction of cement (V_c/V_{cp}) for both of normal concrete (MC-NA) and lightweight aggregate concrete (MC-LC).

ii) The relative initiation stress (σ_{in}/F_{cc}) of normal concrete is not affected by the value of V_c/V_{cp}. However, the value of σ_{in}/F_{cc} of lightweight aggregate concrete increases slightly with the decreasing value of V_c/V_{cp}. This appears to be resulted from that the heterogeneity in concrete becomes smaller as the modulus of elasticity of mortar matrix approaches to that of lightweight aggregate, with the decreasing value of V_c/V_{cp} in the range of $V_c/V_{cp}=0.33$-0.48. The results for the initiation stress of lightweight aggregate concrete in Exp.-Ⅲ. 4. 3 correlated well with results for the progressive microcracking described in Chapter 2.

iii) The relative critical stress (σ_{cr}/F_{cc}) varies with the type of aggregate used. The value of σ_{cr}/F_{cc} of lightweight aggregate concrete is approximately constant, irrespective of the volume fraction of cement (V_c/V_{cp}). On the other hand, the value of σ_{cr}/F_{cc} of normal concrete tends to increase with the increasing value of V_c/V_{cp}, because the modulus of elasticity of mortar matrix approaches to that of river gravel in the range of this experiment, as the value of V_c/V_{cp} is increased.

(2) Empirical equations for characteristic stresses

As described above, the characteristic stresses of concrete are influenced by the volume fractions of cement in cement paste (V_c/V_{cp}), fine aggregate in mortar (V_{sa}/V_m) and coarse aggregate in concrete (V_{ca}/V_{cc}). Therefore, the characteristic stresses of concrete can be generally represented by the following formulas;

$$\sigma_p/F_{cc}=1-{}_pk_c(V_c/V_{cp})-{}_pk_{sa}(V_{sa}/V_m)-{}_pk_{ca}(V_{ca}/V_{cc}) \qquad (3.\ 8)$$

$$\sigma_{in}/F_{cc}=1-{}_ik_c(V_c/V_{cp})-{}_ik_{sa}(V_{sa}/V_m)-{}_ik_{ca}(V_{ca}/V_{cc}) \quad (3.\ 9)$$

$$\sigma_{cr}/F_{cc}=1-{}_ck_c(V_c/V_{cp})-{}_ck_{sa}(V_{sa}/V_m)-{}_ck_{ca}(V_{ca}/V_{cc}) \quad (3.\ 10)$$

where, ${}_pk_c$, ${}_ik_c$, ${}_ck_c$: empirical constants related to the volume fraction of cement
${}_pk_{sa}$, ${}_ik_{sa}$, ${}_ck_{sa}$: empirical constants related to the volume fraction of fine aggregate
${}_pk_{ca}$, ${}_ik_{ca}$, ${}_ck_{ca}$: empirical constants related to the volume fraction of coarse aggregate

The empirical constants in these equations represent the degree of the effect of volume fractions of cement, fine aggregate or coarse aggregate on the characteristic stresses of concrete. Therefore, they are called the "influence factors" for the characteristic stresses in the present paper.

Eqs. (3. 8) through (3. 10) must be consistent with the empirical equations for cement paste and mortar, when V_{ca}/V_{cc} and V_{sa}/V_m equal to zero and V_{ca}/V_{cc} equals to zero, respectively. Therefore, the values of ${}_pk_c$, ${}_ik_c$, ${}_ck_c$, ${}_pk_{sa}$, ${}_ik_{sa}$, and ${}_ck_{sa}$ can be obtained by Eqs. (3. 5) through (3. 7). On the other hand, Eqs. (3. 8) through (3. 10) are rewritten as follows by using the empirical equations (3. 5) through (3. 7).

$$\sigma_p/F_{cc}=\sigma_p/F_{cm}-{}_pk_{ca}(V_{ca}/V_{cc}) \quad (3.\ 11)$$

$$\sigma_{in}/F_{cc}=\sigma_{in}/F_{cm}-{}_ik_{ca}(V_{ca}/V_{cc}) \quad (3.\ 12)$$

$$\sigma_{cr}/F_{cc}=\sigma_{cr}/F_{cm}-{}_ck_{ca}(V_{ca}/V_{cc}) \quad (3.\ 13)$$

Accordingly, the values of ${}_pk_{ca}$, ${}_ik_{ca}$ and ${}_ck_{ca}$ can be represented by

$${}_pk_{ca}=\frac{\sigma_p/F_{cm}-\sigma_p/F_{cc}}{V_{ca}/V_{cc}} \quad (3.\ 14)$$

$${}_ik_{ca}=\frac{\sigma_{in}/F_{cm}-\sigma_{in}/F_{cc}}{V_{ca}/V_{cc}} \quad (3.\ 15)$$

$${}_ck_{ca}=\frac{\sigma_{cr}/F_{cm}-\sigma_{cr}/F_{cc}}{V_{ca}/V_{cc}} \quad (3.\ 16)$$

The values of right side in Eqs. (3. 14) through (3. 16) can be calculated by using the observed values in Exp.-Ⅲ. 2 and Ⅲ. 4. Therefore, the values of ${}_pk_{ca}$, ${}_ik_{ca}$ and ${}_ck_{ca}$ can be obtained.

Finally, these empirical constants could be expressed by the following equations for normal concrete and lightweight aggregate concrete.

For normal concrete;

$${}_pk_{ca}=0.7-1.2(V_c/V_{cp}) \quad (3.\ 17)$$

$${}_ik_{ca}=0.3 \quad (3.\ 18)$$

$${}_ck_{ca}=0.7-1.3(V_c/V_{cp}) \quad (3.\ 19)$$

For lightweight aggregate concrete;

$${}_pk_{ca}=0.7-1.2(V_c/V_{cp}) \quad (3.\ 20)$$

$${}_ik_{ca}=-0.8+2.5(V_c/V_{cp}) \quad (3.\ 21)$$

$$_{c}k_{ca}=0.3 \tag{3. 22}$$

Accordingly, all the influence factors in Eqs. (3. 8) through (3. 10) were determined and the empirical equations for the characteristic stresses of concrete are represented as follows:

For normal concrete;

$$\sigma_p/F_{cc}=1-0.5(V_c/V_{cp})-0.3(V_{sa}/V_m)-[0.7-1.2(V_c/V_{cp})] \times(V_{ca}/V_{cc}) \tag{3. 23}$$

$$\sigma_{in}/F_{cc}=1-0.35(V_{sa}/V_m)-0.3(V_{ca}/V_{cc}) \tag{3. 24}$$

$$\sigma_{cr}/F_{cc}=1-0.05(V_{sa}/V_m)-[0.7-1.3(V_c/V_{cp})](V_{ca}/V_{cc}) \tag{3. 25}$$

For lightweight aggregate concrete;

$$\sigma_p/F_{cc}=1-0.5(V_c/V_{cp})-0.3(V_{sa}/V_m)-[0.7-1.2(V_c/V_{cp})] \times(V_{ca}/V_{cc}) \tag{3. 26}$$

$$\sigma_{in}/F_{cc}=1-0.35(V_{sa}/V_m)-[-0.8+2.5(V_c/V_{cp})](V_{ca}/V_{cc}) \tag{3. 27}$$

$$\sigma_{cr}/F_{cc}=1-0.05(V_{sa}/V_m)-0.3(V_{ca}/V_{cc}) \tag{3. 28}$$

The above equations may be called the general equations for the characteristic stresses of concrete, including the variables related to mix proportions of concrete.

(3) Application of empirical equations for characteristic stresses of concrete

As described previously, test results for the characteristic stresses of concrete vary extremely with investigators and the reason for this conflict has been left unknown. However, this reason can be explained by applying Eqs. (3. 23) through (3. 25).

Table 3. 6 indicates the mix proportions and the characteristic stresses of normal concrete observed by Exp.-Ⅲ. 4. 1 and Ⅲ. 4. 4 in the present chapter, and by Kato[27] and Okushima et al.[41], together with the calculated characteristic stresses by Eqs. (3. 23) through (3. 25). In Exp.-Ⅲ. 4. 4 and Kato's experiment, the volume fractions of fine aggregate (V_{sa}/V_m) and coarse aggregate (V_{ca}/V_{cc}) were varied with W/C. While, in Exp.-Ⅲ. 4. 1 and Okushima's experiment, the volume fraction of coarse aggregate (V_{ca}/V_{cc}) was kept to constant. As indicated in Table 3. 6, the relative proportional limit (σ_p/F_{cc}) and the relative initiation stress (σ_{in}/F_{cc}) obtained by Exp.-Ⅲ. 4. 4 and Kato's experiment decrease with the increasing value of W/C. On the other hand, the value of σ_p/F_{cc} and σ_{in}/F_{cc} obtained by Exp.-Ⅲ. 4. 1 and Okushima's experiment slightly increase with the increasing value of W/C. These observed values were in good agreement with the calculated values. That is, the characteristic stresses of concrete decrease or increase, according to the mix proportions.

(4) Effect of type of coarse aggregate

Figs. 3. 13 through 3. 15 show the relation between σ_p/F_{cc}, σ_{in}/F_{cc} and σ_{cr}/F_{cc}, and V_{ca}/V_{cc} obtained by Exp.-Ⅲ. 3 for PC-series concrete made with cement paste matrix and river gravel (NA), crushed sandstone (SA) or limestone (LI) with 15-20 mm size range, and glass beads (G) or steel ball (S) with 18 mm particle size. The influence factors of coarse aggregate in these concretes represented by

Table 3. 6. Characteristic stresses observed by various investigators.

Investigators	Mix proportion				Calculated value			Observed value			Observed/Calculated		
	W/C	V_c/V_{cp}	V_{sa}/V_m	V_{ca}/V_{cc}	σ_p/F_{cc}	σ_{in}/F_{cc}	σ_{cr}/F_{cc}	σ_p/F_{cc}	σ_{in}/F_{cc}	σ_{cr}/F_{cc}	σ_p/F_{cc}	σ_{in}/F_{cc}	σ_{cr}/F_{cc}
Kato[27]	0.41	0.44	0.35	0.41	0.56	0.75	0.93	0.64	0.81	0.87	1.14	1.08	0.94
	0.49	0.39	0.42	0.45	0.53	0.75	0.89	0.52	0.80	0.89	0.98	1.07	1.00
	0.59	0.35	0.46	0.48	0.50	0.70	0.86	0.53	0.73	0.75	1.06	1.04	0.87
	0.87	0.27	0.51	0.50	0.48	0.68	0.80	0.52	0.73	0.80	1.08	1.07	1.00
Authors Exp.-Ⅲ. 4. 4	0.45	0.41	0.46	0.39	0.54	0.72	0.91	0.52	0.68	0.91	0.96	0.94	1.00
	0.50	0.39	0.50	0.39	0.53	0.71	0.90	0.49	0.65	0.92	0.92	0.92	1.02
	0.55	0.37	0.52	0.39	0.52	0.70	0.89	0.51	0.68	0.87	0.98	0.97	0.98
	0.60	0.35	0.54	0.39	0.51	0.69	0.88	0.47	0.70	0.89	0.92	1.01	1.01
	0.65	0.33	0.56	0.39	0.51	0.69	0.87	0.47	0.65	0.87	0.92	0.94	1.00
	0.70	0.31	0.57	0.36	0.51	0.69	0.86	0.43	0.64	0.86	0.84	0.95	1.00
Okushima et al.[41]	0.45	0.41	0.55	0.40	0.50	0.69	0.90	—	0.67	0.88	—	0.97	0.98
	0.65	0.33	0.55	0.40	0.51	0.69	0.87	—	0.73	0.93	—	1.06	1.07
	0.75	0.30	0.55	0.40	0.52	0.69	0.85	—	0.78	0.91	—	1.13	1.07
Authors Exp.-Ⅲ. 4. 1	0.45	0.41	0.51	0.30	0.55	0.73	0.92	0.57	0.72	0.89	1.04	0.99	0.97
	0.55	0.37	0.48	0.30	0.56	0.74	0.91	0.58	0.75	0.84	1.04	1.01	0.92
	0.70	0.31	0.44	0.30	0.58	0.76	0.89	0.60	0.76	0.81	1.03	1.00	0.91

Eqs. (3. 14) through (3. 16) and the modulus of elasticity (E_a) of the above aggregates are given in Table 3. 7. As shown in Figs. 3. 13 through 3. 15 and Table 3. 7, the relative initiation stress (σ_{in}/F_{cc}) and the relative critical stress (σ_{cr}/F_{cc}) were usually smaller the larger the modulus of elasticity of aggregate. Especially, each of characteristic stresses of concrete made with steel ball aggregate (PC-S specimen) were considerably smaller than those of concretes made with river gravel or crushed limestone (PC-NA or PC-LI specimen, respectively). This is probably caused from that the heterogeneity in concrete increases as the difference of elastic moduli in coarse aggregate and matrix is increased. On the other hand, the value of ${}_pk_{ca}$, i.e., the influence factor of coarse aggregate for the proportional limit of concrete made with crushed limestone aggregate (PC-LI specimen) is considerably smaller than that of concrete made with river gravel (PC-NA specimen), although the modulus of elasticity of crushed limestone is approximately equal to that of river gravel. This phenomenon can be explained as follows: The bond between coarse aggregate and cement paste matrix for PC-LI specimen is strengthened by the chemical bonding effect between cement paste and silica in the limestone. Therefore, the initiation of bond cracks in PC-LI specimen was delayed, compared with PC-NA specimen.

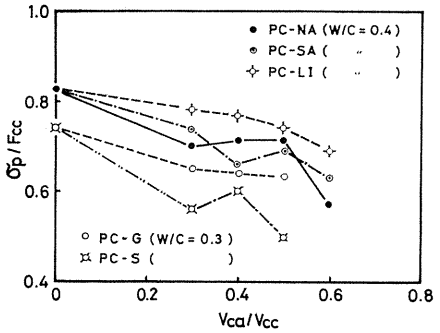

Fig. 3. 13. Effect of type of coarse aggregate on relative proportional limit (σ_p/F_{cc}) of PC-series concrete.

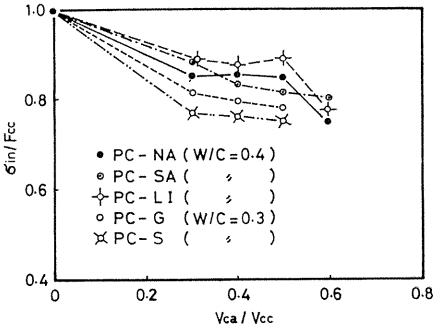

Fig. 3. 14. Effect of type of coarse aggregate on relative initiation stress (σ_{in}/F_{cc}) of PC-series concrete.

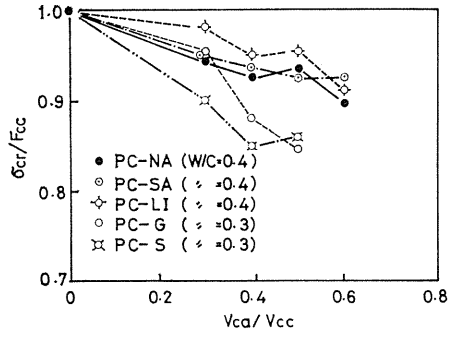

Fig. 3. 15. Effect of type of coarse aggregate on relative critical stress (σ_{cr}/F_{cc}) of PC-series concrete.

Table 3. 7. Influence factor due to coarse aggregate.

Type of coarse aggregate	Notation	E_a (kg/cm^2)	$_pk_{ca}$	$_ik_{ca}$	$_ck_{ca}$
River gravel	NA	6.57×10^5	0.33	0.38	0.17
Limestone	LI	5.72×10^5	0.20	0.31	0.11
Sandstone	SA	6.24×10^5	0.33	0.36	0.13
Glass beads	G	(7×10^5)	0.24	0.52	0.26
Steel ball	S	(21×10^5)	0.46	0.59	0.33

(5) Effect of size of aggregate

Figs. 3. 16 and 3. 17 indicate the relation between the relative characteristic stresses (σ/F_{cc}) and the size of aggregate (ϕ_a). As shown in these figures, each of characteristic stresses of concrete is fairly smaller than that of cement paste illustrated at $\phi_a=0$. However, the decrease rate of the relative characteristic stresses with the increasing size of aggregate is relatively small. In general, with the increasing size of aggregate, bleeding beneath the coarse aggregate particles increases[58] and the bond cracks begin to propagate at the smaller stress level. Therefore, it is considered that the characteristic stresses, such as proportional limit (σ_p) become smaller with the increasing size of aggregate. On the other hand, with the increasing size of aggregate, the area of interface between coarse aggregate and matrix decreases for the concrete with a constant volume fraction of coarse aggregate, that is, the possibility of the occurrence of bond cracks become smaller. Therefore, it seems that the characteristic stresses becomes larger with the increasing size of aggregate.

The fact that the relative characteristic stresses decreased with the increasing size of aggregate may be caused by that the effect of the former is dominant, compared with that of the latter.

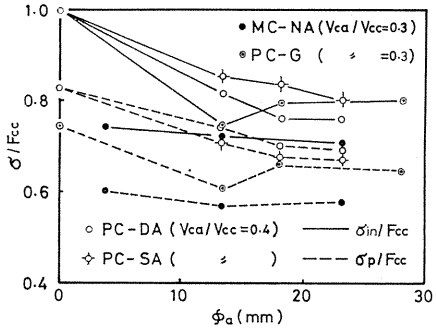

Fig. 3. 16. Effect of size of aggregate (ϕ_a) on relative proportional limit (σ_p/F_{cc}) and relative initiation stress (σ_{in}/F_{cc}).

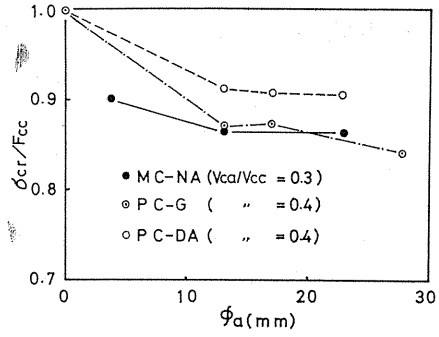

Fig. 3. 17. Effect of size of aggregate (ϕ_a) on relative critical stress (σ_{cr}/F_{cc}).

(6) Effect of end condition of specimen

As described in Chapter 2, critical stress approximately coincides with the stress at which the long continuous cracks are formed. Consequently, when the frictional restraint effect of the ends of specimen is eliminated, it is expected that the specimen fails simultaneously at the formation of continuous cracks. This expectation was ascertained in Exp.-Ⅲ. 4. 1. Fig. 3. 18 indicates the stress (σ)-strain (ε) curves of PA-series specimen which was loaded by inserting the lubricating pads between the ends of specimen and the loading platens, and NO-series specimen which was loaded under the normal loading condition specified in JIS A 1108. As shown in Fig. 3. 18, the stress-strain curves of both specimens are hardly different at the lower stress than the critical stress (σ_{cr}). At the higher stress than the critical stress, NO-series specimen can sustain the load, but PA-series specimen failed simultaneously at the critical stress.

Fig. 3. 19 shows the relation between ${}_pF_c/F_{cc}$ and σ_{cr}/F_{cc}, where, ${}_pF_c$ and F_{cc} are the compressive strengths of PA-series specimen and NO-series specimen, respectively. The compressive strength of PA-series specimen is approximately consistent with the critical stress of NO-series specimen. Accordingly, it may be concluded that the critical stress is a basic characteristic property of concrete which is not affected by the loading method.

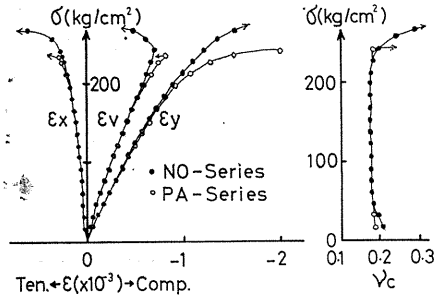

Fig. 3. 18. Effect of end condition of specimen on stress (σ) - strain (ε) and stress (σ) - Poisson's ratio (ν_c) relations.

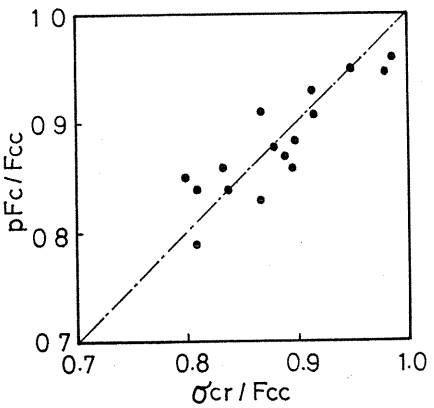

Fig. 3. 19. Relation between relative compressive strength ($_pF_c/F_{cc}$) of PA-series specimen and relative critical stress (σ_{cr}/F_{cc}) of NO-series specimen.

3. 4. Conclusion

In this chapter, the fracture process of concrete was represented indirectly by the characteristic stresses, such as proportional limit, initiation stress and critical stress on the stress-strain curve of concrete, and the effect of various factors related to aggregate and matrix was examined by a series of experiments.

The main results obtained in the present chapter are summarized as follows:

1) The ratio of the proportional limit to the compressive strength of cement paste (σ_p/F_{cp}) decreases with the increasing volume fraction of cement in cement paste (V_c/V_{cp}), but the initiation stress and the critical stress of cement paste

approximately coincide with the compressive strength.

2) The ratio of the proportional limit to the compressive strength of mortar (σ_p/F_{cm}) decreases with the increasing volume fractions of cement in cement paste (V_c/V_{cp}) and fine aggregate in mortar (V_{sa}/V_m). On the other hand, the ratios of the initiation stress and the critical stress to the compressive strength of mortar (σ_{in}/F_{cm} and σ_{cr}/F_{cm}, respectively) decrease with the increasing value of V_{sa}/V_m.

3) The ratios of the proportional limit, the initiation stress and the critical stress to the compressive strength of concrete (σ_p/F_{cc}, σ_{in}/F_{cc} and σ_{cr}/F_{cc}, respectively) decrease with the increase of volume fractions of coarse aggregate in concrete (V_{ca}/V_{cc}) and fine aggregate in mortar matrix (V_{sa}/V_m). The effect of V_c/V_{cp} on these characteristic stresses varies with the type of coarse aggregate used and the mix proportions. The relative characteristic stresses of concrete decrease or increase according to the change of mix proportions.

4) The relative characteristic stresses (σ_p/F_{cc}, σ_{in}/F_{cc} and σ_{cr}/F_{cc}) are represented by the empirical equations (3. 23) through (3. 25) for normal concrete and (3. 26) through (3. 28) for lightweight aggregate concrete. These equations are also applicable to estimating the characteristic stresses of cement paste and mortar, when the values of V_{ca}/V_{cc} and V_{sa}/V_m equal to zero and the value of V_{ca}/V_{cc} equals to zero, respectively.

5) The difference of test results for the characteristic stresses of concrete obtained by previous investigators was resulted from the difference in the mix proportions of concrete used in each of investigations.

6) The relative characteristic stresses (σ_p/F_{cc}, σ_{in}/F_{cc} and σ_{cr}/F_{cc}) increase as the elastic modulus of matrix approaches to that of coarse aggregate.

7) The critical stress of concrete obtained under the normal testing condition specified in JIS A 1108 correlates well with the compressive strength of concrete obtained under the test in which the frictional restraint effect of the ends of specimen is eliminated.

4. Model Analysis of Fracture and Failure of Concrete

4. 1. Introduction

There have been many attempts over the years to explain the mechanical properties of concrete with the help of various structural and interparticle models[59)~62)]. Especially in recent years, many structural models for the examination of mechanical properties of concrete under uniaxial compression have been proposed, as shown in Table 1.1.[43)~55)] Among them, Shah and Winter[43)] have used a prismatic mortar specimen having a cylindrical aggregate, and pointed out that the progressive microcracking in concrete at the structural level closely relates to the particular shape of the stress-strain curve of concrete at the phenomenological level. Wischers and Lusche[53)] have used a prismatic plate model having two cylindrical or prismatic aggregates, and found that the stress concentration in concrete is noticeably affected by the shape of aggregate and the clear distance between two aggregates. Buyukozturk, Nilson and Slate[49)] have indicated that the bond cracks initiate at the load of about 45 percent of ultimate and are interconnected to mortar cracks at the load of about 82 percent of ultimate, by using the model having nine cylindrical

aggregates embedded regularly in mortar matrix. Liu, Nilson and Slate[23] have applied a plate model embedded many aggregates randomly, and obtained the following results: 1) Bond cracks initiate at the load of about 65 percent of ultimate, 2) mortar cracks bridge between bond cracks to form the continuous crack patterns at the load of about 85 percent of ultimate, and 3) the specimen shows the splitting failure caused by the longitudinal continuous cracks.

As described above, there have been many investigations used the structural models but in most of investigations, a fixed quality of aggregate was applied. Therefore, few studies have examined in detail the effect of the mechanical properties of aggregate on the fracture and failure of concrete by the model analysis.

In addition to the studies used a simplified model specimen as described above, there have been several investigations in which were used ordinary shaped concrete specimens having various model aggregates with known qualities and were examined the effect of the mechanical properties and the surface texture of aggregate on the properties of concrete[45)54)55)63)64)]. Among the investigators who have examined the effect of the surface condition of coarse aggregate on the compressive strength of concrete, Darwin and Slate[63] and Soshiroda et al.[58] have found this effect to be negligible, while Nepper-Christensen and Nielsen[64] and authors[55] have indicated this effect to be noticeable.

On the other hand, Okajima[54] and authors[44] have ascertained that the compressive strength of concrete is affected by the modular ratio of mortar matrix and coarse aggregate. But a detailed examination for this reason has not been made.

The main object of the present chapter is to examine the effect of the mechanical properties and the surface condition of coarse aggregate on the fracture and failure of concrete. This chapter is characterized by using a simplified model with an aggregate made of mortar whose mechanical properties and surface condition can be easily changed.

4. 2. Test procedure

4. 2. 1. Outline of experiments

The following three series and five kinds of experiment were conducted in the present chapter. Outline of the experiments is shown in Tables 4. 1. 1 through 4. 1. 3.

1) Experiment-Ⅳ. 1; The object of Exp.-Ⅳ. 1 is to examine the bond properties between mortar matrix and coarse aggregate and to obtain fundamental data for analyzing the test results of Exp.-Ⅳ. 2 described later. In Exp.-Ⅳ. 1. 1, the effects of the water-cement ratio (W/C) and the surface condition of coarse aggregate on the flexual bond strength were examined. The specimen and the loading method in Exp.-Ⅳ. 1. 1 are shown in Fig. 4. 1. 1. Five types of surface condition of aggregate were prepared, as shown in Table 4. 2. The thickness of epoxy resin used in B-series specimen with a bonded aggregate was kept to about 1 mm.

On the other hand, the shear-compressive bond strength between mortar matrix and aggregate was obtained in Exp.-Ⅳ. 1. 2, by using $4\times4\times16$ cm prismatic specimen shown in Fig. 4. 1. 2. The variables in Exp.-Ⅳ. 1. 2 are as follows: five kinds of θ (the angle of inclination of the interface between mortar matrix and aggregate to the lateral axis of specimen), three kinds of W/C and four kinds of surface condition of aggregate (N-series, B-series, R-series and P-series in Table 4. 2).

Table 4. 1. Outline of experiments.

Table 4. 1. 1. Experiment-Ⅳ. 1.

Notation of experiment	Surface condition of aggregate[1)]	W/C of matrix	W/C (S/C[2)]) of aggregate	θ (deg.)[3)]
Exp.-Ⅳ. 1. 1	N, O, B, R, P	0.6	0.3 (0.2) 0.6 (2.0) 0.9 (3.5)	—
Exp.-Ⅳ. 1. 2	N, R, P	0.6	0.3 (0.2) 0.6 (2.0) 0.9 (3.5)	30, 45, 55, 65, 75
	B	0.6	0.6 (2.0)	15, 30, 45, 60, 75

[Notation] 1) see Table 4. 2.
2) Sand-cement ratio by weight.
3) Angle of inclination of boundary layer to horizontal plane.

Table 4. 1. 2. Experiment-Ⅳ. 2.

Notation of experiment	Surface condition of aggregate	W/C of matrix	Type of aggregate	W/C of aggregate
Exp.-Ⅳ. 2. 1	N, R, P	0.6	Mortar Mortar Mortar	0.3 0.6 0.9
Exp.-Ⅳ. 2. 2	N, O, B	0.6	Mortar Mortar Mortar Steel	0.3 0.6 0.9 —

Table 4. 1. 3. Experiment-Ⅳ. 3.

Notation of specimen	W/C of aggregate	V_{ca}/V_{cc}[1)]	W/C (V_{sa}/V_a[2)]) of matrix
MC-MH	0.40	0.3	0.30 (0.11), 0.35 (0.28), 0.40 (0.57) 0.45 (0.59), 0.55 (0.61) 0.65 (0.62), 0.75 (0.63)
MC-ML	0.55		

[Notation] 1) Volume fraction of coarse aggregate.
2) Ratio of fine aggregate to total aggregate by volume.

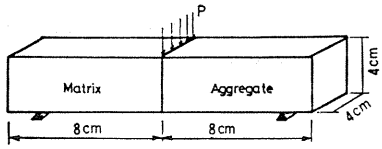

Fig. 4. 1. 1. Exp.-Ⅳ. 1. 1

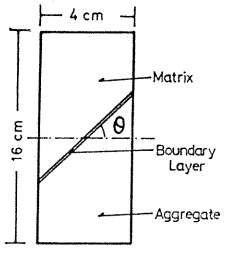

Fig. 4. 1. 2. Exp.-Ⅳ. 1. 2

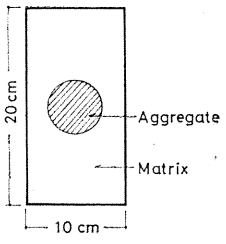

Fig. 4. 1. 3. Exp.-Ⅳ. 2

Fig. 4. 1. Specimen.

Table 4. 2. Surface condition of mortar aggregate.

Notation of specimen	Type of specimen
N-series	Specimen having an aggregate with a normal surface texture which has been left alone after removed from the mold until being cast in mortar matrix
O-series	Specimen having an aggregate whose surface is covered with a polyethylene sheet (20μ in thickness) to eliminate the bonding effect between mortar matrix and aggregate
B-series	Specimen having an aggregate adhered to mortar matrix by epoxy resin
R-series	Specimen having an aggregate with a jagged surface (1mm in depth and 1.5 mm in distance of jaggedness)
P-series	Specimen having an aggregate whose surface is ground by sand-paper (#80)

2) Experiment-Ⅳ. 2; The object of Exp.-Ⅳ. 2 is to examine the effect of the mechanical properties and the surface condition of aggregate on the fracture and failure of model concrete. Prismatic model concretes of 5×10 cm in section and 20 cm in height embedded a cylindrical mortar aggregate of 5 cm in diameter in mortar matrix were prepared. Three kinds of water-cement ratio (W/C) were chosen for mortar aggregate, while the value of W/C for mortar matrix was kept to 0. 6.

Exp.-Ⅳ. 2 was subdivided into Exp.-Ⅳ. 2. 1 and Exp.-Ⅳ. 2. 2. In Exp.-Ⅳ. 2. 1, N-series, R-series and P-series (see Table 4. 2) were applied and in Exp.-Ⅳ. 2. 2, N-series, B-series and O-series (see Table 4. 2) were applied for the surface condition of coarse aggregate. That is, the bond properties between mortar matrix and aggregate in Exp.-Ⅳ. 2. 1 and Exp.-Ⅳ. 2. 2 were changed by changing the surface roughness of aggregate and by inserting a different material from mortar matrix or aggregate between them, respectively.

H-series specimen, i. e., the specimen with a cylindrical hole of 5 cm in diameter in the central portion of specimen was also prepared in Exp.-Ⅳ. 2.

3) Experiment-Ⅳ. 3; The object of Exp.-Ⅳ. 3 is to examine the effect of the mechanical properties of coarse aggregate on the compressive strength of concrete. The cylindrical specimen of 10 cm in diameter and 20 cm in height was used and the spherical mortar aggregate of about 2 cm in diameter was prepared for coarse aggregate. The aggregate was made by grinding the edges of 2 cm mortar cube. The volume fraction of coarse aggregate in concrete was kept to 0. 3. The variables of Exp.-Ⅳ. 3 are as follows: two kinds of W/C of mortar aggregate and seven kinds of W/C of mortar matrix as shown in Table 4. 1. 3.

4. 2. 2. Fabrication and curing of specimen

(1) Materials used

i) Cement; High-early strength Portland cement was used. The compressive strength of cement was 398-422 kg/cm^2 at the age of 28 days.

ii) Fine aggregate; Kiso-river sand (maximum size = 2.5 mm, specific gravity = 2.59, fineness modulus = 1.99, water absorption at 24 hours = 2.1 percent) was prepared for fine aggregate.

iii) Coarse aggregate; Mortar aggregate was used as coarse aggregate. In addition, steel aggregate was also used in Exp.-Ⅳ. 2. 2. The compressive strength (F_c), tensile splitting strength (F_t) and modulus of elasticity (E) at a stress level of one-third the compressive strength obtained by $\phi 10\times 20$ cm cylinders are shown in Table 4. 3. Subscripts "m" and "a" in Table 4. 3 represent mortar matrix and aggregate, respectively.

The modulus of elasticity of epoxy resin used for adhering the aggregate to mortar matrix in B-series specimen was of the order of 4×10^3 to 7×10^3 kg/cm^2 at the age of test.

Table 4. 3. Mechanical properties of mortar matrix and aggregate.

Notation of experiment	Matrix				Aggregate				F_{ca}/F_{cm}	E_a/E_m
	W/C	F_{cm} (kg/cm^2)	F_{tm} (kg/cm^2)	E_m (kg/cm^2)	W/C	F_{ca} (kg/cm^2)	F_{ta} (kg/cm^2)	E_a (kg/cm^2)		
Exp.-Ⅳ. 1. 2	0.6	279	23.0	2.05×10^5	0.3	557	38.2	2.47×10^5	2.00	1.20
Exp.-Ⅳ. 2. 1		290	26.2	1.89×10^5	0.6	292	27.0	1.92×10^5	1.01	1.02
		260	26.3	1.92×10^5	0.9	161	13.1	1.06×10^5	0.62	0.55
Exp.-Ⅳ. 1. 1	0.6	252	23.5	2.00×10^5	0.3	640	44.0	2.74×10^5	2.57	1.37
Exp.-Ⅳ. 2. 2		259	24.8	2.07×10^5	0.6	269	25.6	2.08×10^5	1.04	1.01
		242	21.0	1.96×10^5	0.9	104	11.9	1.19×10^5	0.43	0.61
		250	22.3	2.12×10^5	(Steel)	—	—	(21.0×10^5)	—	(10.3)
Exp.-Ⅳ. 3	0.30	632	42.0	2.65×10^5	0.40	465	36.5	2.48×10^5	—	—
	0.35	530	37.2	2.52×10^5						
	0.40	461	36.0	2.31×10^5						
	0.45	389	30.3	2.21×10^5						
	0.55	308	27.0	1.98×10^5	0.55	318	25.2	2.05×10^5	—	—
	0.65	249	23.1	1.93×10^5						
	0.75	204	20.1	1.75×10^5						

[Subscript] m: Matrix. a: Aggregate

(2) Fabrication and curing of specimen

The procedure of the fabrication of specimens in Exp.-Ⅳ. 2 is as follows: Mortar matrix was cast in steel mold after a cylindrical aggregate was carefully fixed to the central portion of mold. The direction of casting was vertical to the loading axis. In Exp.-Ⅳ. 3, the following procedure was applied to keep the volume fraction of coarse aggregate in concrete to the fixed value. Initially, mortar matrix was mixed by a pan-type mixer. The coarse aggregate corresponding to the volume fraction in a $\phi 10\times 20$ cm concrete cylinder and the premixed mortar matrix were again mixed by hand and cast in steel mold.

All specimens were cured in the room at a temperature of $20°\pm 1°$C and a relative humidity of 90 ± 5 percent until the tests. The tests were carried out at the age of 7 days of mortar matrix (corresponding to the age of 10 days of mortar

aggregate).

4. 2. 3. Methods of loading and measurement

The specimens were loaded in a hydraulic testing machine and the loading rate was kept to about 2-3 kg/cm^2/sec. up to the failure of specimens. In Exp.-Ⅳ. 2, the lubricating pads described in Chapters 2 and 3 were interposed between the ends of specimen and the loading platens, to minimize the restraint effect of the lateral deformation of specimen.

67 mm and 10 mm length wire strain gages were applied for the measurement of strain distribution in the specimen.

4. 3. Test results and discussion

4. 3. 1. Bond strength between mortar matrix and coarse aggregate

(1) Flexual bond strength

Fig. 4. 2 indicates the relation between F_b and W/C obtained by Exp.-Ⅳ. 1. 1, where, F_b and W/C are the flexual bond strength between mortar matrix and aggregate and the water-cement ratio of mortar aggregate, respectively. As shown in Fig. 4. 2, the flexual bond strength (F_b) is hardly affected by the value of W/C but varies noticeably with the surface condition of aggregate. That is, the flexual bond strengths of B-series specimen with a bonded aggregate, R-series specimen with a rough-textured aggregate, N-series specimen with a normal-textured aggregate and P-series specimen with a smooth-textured aggregate were about 24-26, 18-21, 13-16 and 12-15 kg/cm^2, respectively. The flexual bond strength of O-series specimen with a bond-reduced aggregate was negligible.

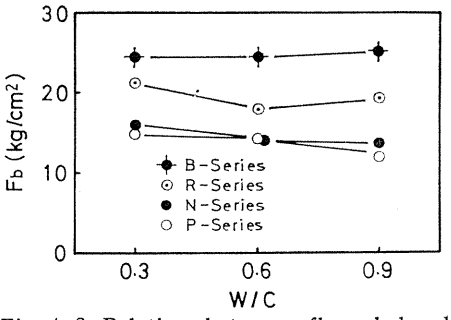

Fig. 4. 2. Relation between flexual bond strength (F_b) and water-cement ratio of mortar aggregate (W/C).

(2) Shear-compressive bond strength

R-series, N-series, B-series and P-series specimens with various inclination angles (θ) of the interface between aggregate and mortar matrix were uniaxially compressed to obtain the bond strength under combined compression and shear. The relations between τ_n and σ_n obtained by Exp.-Ⅳ. 1. 2 are given in Figs. 4. 3. 1 through 4. 3. 3, where, τ_n and σ_n are the tangential stress and the normal stress at the interface, respectively. The figures of 30, 60 and 90 in Fig. 4. 3 represent the percentages of water-cement ratio of mortar aggregate. As indicated in Fig. 4. 3, the relation between τ_n and σ_n can be approximately expressed by the following formula.

$$\tau_n = c - \tan\phi \cdot \sigma_n \qquad (4.\ 1)$$

where, c and ϕ are empirical constants generally termed cohesive strength and angle of friction, respectively.

The observed values of c and ϕ in Eq. (4. 1) are indicated in Table 4. 4. As indicated in Table 4. 4, the observed angle of friction (ϕ) is largest in R-series specimen with a rough-textured aggregate and is smallest in B-series specimen with

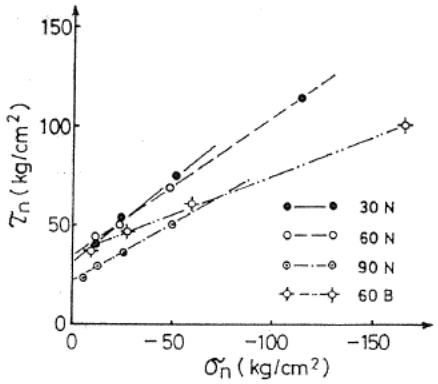

Fig. 4. 3. 1. N-series and B-series specimens.

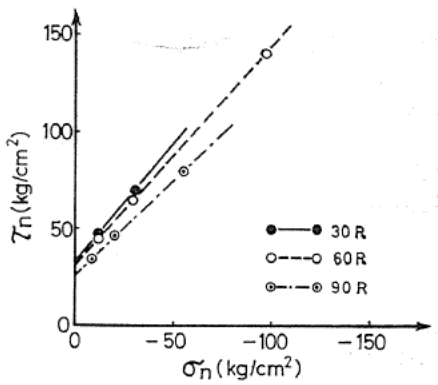

Fig. 4. 3. 2. R-series specimen.

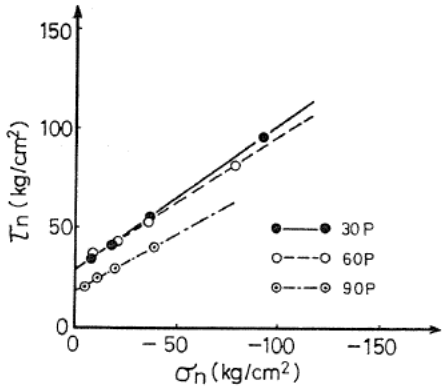

Fig. 4. 3. 3. P-series specimen.

Fig. 4. 3. Relation between shear stress (τ_n) and normal stress (σ_n) at the interface between aggregate and mortar matrix at failure.

a bonded aggregate at a given water-cement ratio of mortar aggregate. Besides the value of ϕ slightly decreases with the increasing value of W/C at a given surface condition of aggregate.

On the other hand, the cohesive strength (c) of the specimens with $W/C=0.3$ is approximately equal to that of the specimens with $W/C=0.6$. This may be resulted from that the water-cement ratio of mortar matrix was kept to 0.6 and

Table 4. 4. Measured values of c and ϕ (Exp.-Ⅳ. 2).

Surface condition of aggregate	$W/C=0.3$		$W/C=0.6$		$W/C=0.9$	
	c (kg/cm²)	ϕ (deg.)	c (kg/cm²)	ϕ (deg.)	c (kg/cm²)	ϕ (deg.)
N-series	32	33	35	34	22	30
B-series	—	—	35	22	—	—
R-series	33	51	30	48	26	45
P-series	29	36	29	33	18	30

the sliding failure at the interface of both specimens was mainly dependent on the failure of mortar matrix.

The sliding at the interface was not appeared in N-series, P-series and R-series specimens with $\theta=30$ deg. and in B-series specimen with $\theta=15$ deg.

The relative deformation between mortar matrix and aggregate was measured by a microscope with 100 powers magnification and wire strain gages, but was not appeared prior to the sliding failure of specimen.

4. 3. 2. Stress-strain relation of model concrete

It is important for understanding the fracture process of concrete to examine the state of strain at aggregate, mortar matrix and the interface between mortar matrix and aggregate in model concretes under the increasing load.

In the present clause, the effect of the mechanical properties and the surface condition of aggregate on the fracture process of model concrete will be discussed, in terms of the stress-strain relations of model concrete obtained in Exp.-Ⅳ. 2.

Photo. 4. 1 shows the typical fracture mode of model concrete. A few cracks in the photographs occurred after the maximum load.

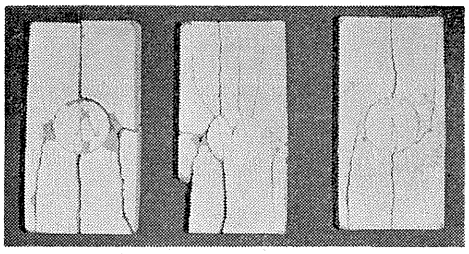

O-series N-series B-series

W/C of aggregate 0.9

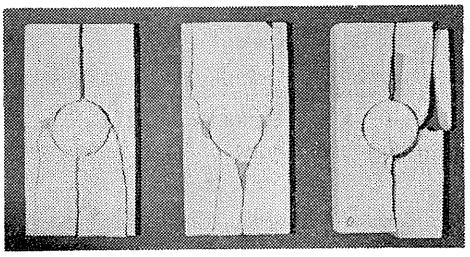

O-series N-series B-series

W/C of aggregate 0.6

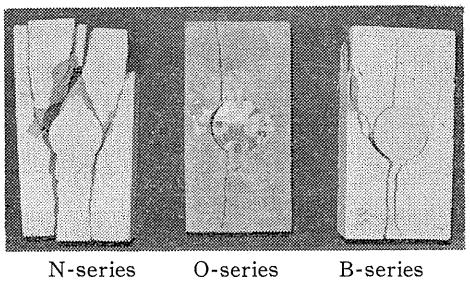

N-series O-series B-series

W/C of aggregate 0.3

Photo. 4. 1. Typical failure mode of model concrete (Exp.-Ⅳ. 2. 2).

(1) Effect of mechanical properties of aggregate

Typical stress (σ) - strain (ε) relations for N-series specimen with a normal-textured aggregate obtained by Exp.-Ⅳ. 2. 1 are shown in Figs. 4. 4. 1 through 4. 4. 3. Hereafter the longitudinal and the lateral directions of specimen are termed y- and x-directions, respectively.

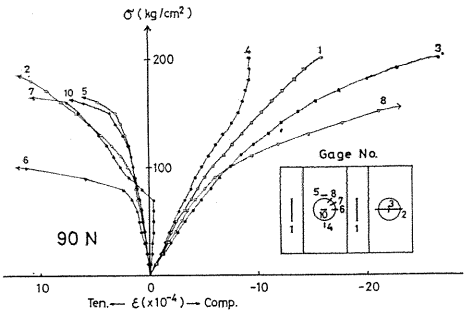

Fig. 4. 4. 1. 90 N-specimen.

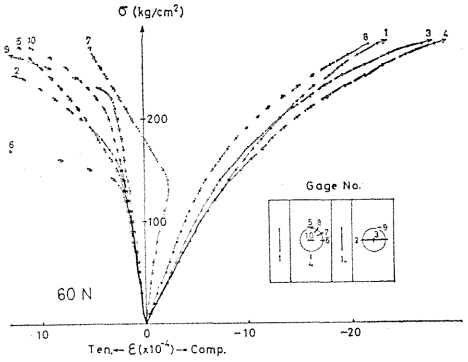

Fig. 4. 4. 2. 60 N-specimen.

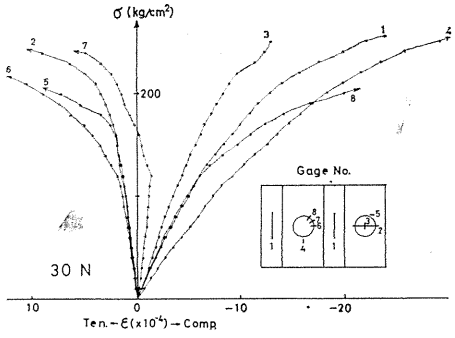

Fig. 4. 4. 3. 30 N-specimen.

Fig. 4. 4. Stress (σ) - strain (ε) relation of model concrete (Effect of quality of aggregate).

The results obtained from Fig. 4. 4 are as follows:

i) Specimen with smaller strength of aggregate than that of mortar matrix (90N-specimen); As shown in Fig. 4. 4. 1, the strains at various locations in the specimen increase linearly with the increasing stress up to the stress smaller than about 80 kg/cm² (corresponding to 40 percent of the compressive strength: F_{cc}) and the largest strain in this range of stress is the strain at the location of Gage No. 3, i. e., the aggregate strain in y-direction. When the stress (σ) becomes larger than 80 kg/cm² (0.40 F_{cc}), the strains of Gage No. 6, No. 7 and No. 8, i. e., the strains at the interface between mortar matrix and aggregate increase rapidly and the bond crack is formed at the interface. At the stress level of about 150 kg/cm² (0.75 F_{cc}), the strains of Gage No. 5, i. e., the mortar strain in x-direction at the location 1 cm distant from the top surface of aggregate and the strain of Gage No. 10, i. e., the aggregate strain in x-direction increase noticeably. Namely, mortar

crack and aggregate crack begin to propagate simultaneously. It can not be decided in Fig. 4. 4. 1 that either of these cracks is first formed in 90 N-specimen. However, it is estimated from a previous paper by authors[57] in which the stress distribution in x-direction of model concrete was examined by the finite element analysis and an experiment, that the mortar crack will first occur and later cause the aggregate crack in 90 N-specimen.

At the stress level larger than 150 kg/cm^2, the strain of Gage No. 3, i. e., the aggregate strain in y-direction increases more rapidly and the local compressive failure in aggregate occurs. Finally, the compressive failure in aggregate appears to cause the whole disruption of 90 N-specimen.

ii) Specimen with nearly equal strength of aggregate and mortar matrix (60 N-specimen); 60 N-specimen was made with a mortar aggregate with the same water-cement ratio as that of mortar matrix. Therefore, it is assumed that 60 N-specimen is primarily homogeneous at the smaller stress level. At the stress level smaller than 120 kg/cm^2 (0.42 F_{cc}), the strains in y-direction (Gage No. 1, 3 and 4) and the strains in x-direction (Gage No, 2, 5, 6, 9 and 10) show approximately indentical values, respectively,

At the stress level of about 120 kg/cm^2 (0.42 F_{cc}), the strain of Gage No. 7, i. e., the strain at the interface between mortar matrix and aggregate begins to increase rather than continuing to decrease under the increasing stress. Simultaneously, the average strain in x-direction (Gage No. 2) increases rapidly and the bond crack begins to propagate.

At the stress level of about 220 kg/cm^2 (0.78 F_{cc}), the increase rate of strain of Gage No. 9, i. e., the mortar strain in x-direction at the vicinity of coarse aggregate becomes larger and the mortar crack occurs at that location. At the stress level larger than 220 kg/cm^2, the local compressive failure in both mortar matrix (Gage No. 4) and aggregate (Gage No. 3) occurs and finally causes the failure of 60 N-specimen.

iii) Specimen with larger strength of aggregate than that of mortar matrix (30 N-specimen); The relations between the stress and the strains at various locations are approximately represented by straight lines at the stress level smaller than about 140 kg/cm^2 (0.54 F_{cc}). At the stress level of about 140 kg/cm^2 (0.54 F_{cc}), the increase rate of the strains of Gage No. 6 and No. 8, i. e., the strains at the interface show considerable changes and bond crack is formed.

At the stress level of about 180 kg/cm^2 (0.70 F_{cc}), the strain of Gage No. 5, i. e., the mortar strain in x-direction at the vicinity of aggregate shows a rapid change and mortar crack is formed. As the stress is more increased, the strain of Gage No. 4, i. e., the mortar strain in y-direction at the vicinity of aggregate becomes very large and it seems that the local compressive failure in mortar matrix causes the failure of 30 N-specimen.

The results described above are summarized as follows:

① Bond crack is the first structural change, regardless of the strength of aggregate. ② For the specimen with smaller strength of aggregate than that of mortar matrix, mortar crack and aggregate crack begin to propagate simultaneously parallel to the longitudinal axis and the local compressive failure in aggregate causes the failure of specimen. ③ For the specimen with nearly equal strength of aggregate and mortar matrix, bond crack at the interface is interconnected to mortar crack and the compressive failure in both aggregate and mortar matrix causes the failure of specimen. ④ For the specimen with larger strength than that of mortar

matrix, bond crack is interconnected to mortar crack parallel to the longitudinal axis and the local compressive failure in mortar matrix at the vicinity of top and bottom surface of aggregate causes the failure of specimen.

As described above, the fracture process of concrete is considerably affected by the mechanical properties of aggregate.

(2) Effect of surface condition of aggregate

Fig. 4. 5 shows the stress (σ) - strain (ε) relations of R-series specimen with a rough-textured aggregate and N-series specimen with a normal-textured aggregate obtained by Exp.-Ⅳ. 2. 1. Both specimens shown in Fig. 4. 5 are consisted of mortar matrix and aggregate with W/C=0.6 and the surface roughness of aggregate varies with them. The stress-strain curves of these specimens show a similar shape, with the exception that the stress at which bond crack begins to propagate varies with the specimens. Especially, the strain of Gage No. 1, i. e., the average strain in y-direction of N-series specimen is hardly different from that of R-series specimen. The stress at the initiation of bond crack for R-series specimen is larger than that for N-series specimen, since the bond strength between aggregate and matrix of R-series specimen is larger as shown in Fig. 4. 3. However, the mechanical properties of mortar matrix and aggregate in both specimens and their topology are approximately identical after the bond crack is formed. The fact that the stress-strain relation is hardly affected by the surface roughness of aggregate may be resulted from the above reason.

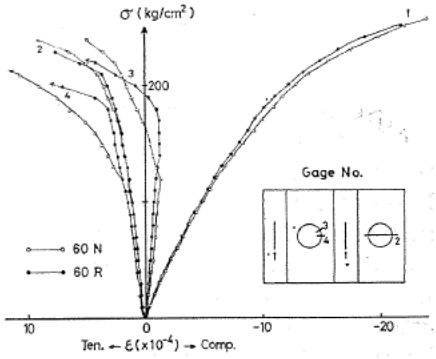

Fig. 4. 5. Stress (σ) - strain (ε) relation of model concrete (Effect of surface condition of aggregate (Exp.-Ⅳ. 2. 1)).

The stress-strain relations for O-series specimen with a bond-reduced aggregate and B-series specimen with a bonded aggregate obtained by Exp.-Ⅳ. 2. 2 are given in Figs. 4. 6. 1 and 4. 6. 2, respectively. The specimens shown in Fig. 4. 6 are also consisted of mortar matrix and aggregate with W/C=0.6. But a different material from mortar matrix or aggregate was interposed between them, so as to change the bond properties. As shown in Fig. 4. 6, the strains at the various locations in both specimens increase linearly at the stress level smaller than about 40 percent of the compressive strength (F_{cc}). The strains of Gage No. 3 and No. 4, i. e., the strains at the interface between mortar matrix and aggregate are very large, while the strains of Gage No. 6 and No. 7, i. e., the aggregate strains are very small in both specimens. Consequently, it can be estimated that the stress is not adequetely transmitted to aggregate in these specimens.

At the stress level of about 60 kg/cm² (0.65 F_{cc}) for O-series specimen and about 40 kg/cm² (0.45 F_{cc}) for B-series specimen, the strain of Gage No.5, i. e., the mortar strain in x-direction at the vicinity of the top and bottom surface of aggregate increases noticeably and the mortar crack is observed at that location. After the stress becomes larger, the strain of Gage No.7, i. e., the aggregate strain in x-direction becomes larger and the splitting in the aggregate was appeared in a few specimens. Finally, these specimens were failed by longitudinal splitting.

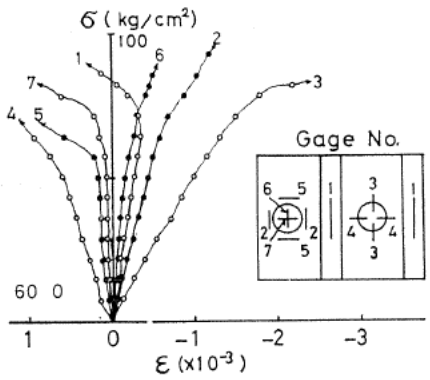

Fig. 4. 6. 1. 60 O-specimen

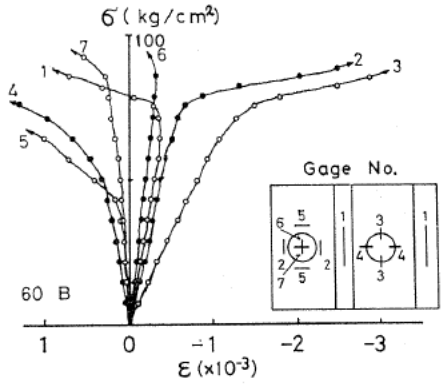

Fig. 4. 6. 2. 60 B-specimen

Fig. 4. 6. Stress (σ) - strain (ε) relation of model concrete (Effect of surface condition of aggregate (Exp.-Ⅳ. 2. 2)).

As described above, the stress-strain relation obtained by Exp.-Ⅳ. 2. 1 was hardly affected by the surface condition of aggregate, but these relations of O-series and B-series specimens obtained by Exp.-Ⅳ. 2. 2 were different from that of N-series specimen. This reason may be explained as follows: In Exp.-Ⅳ. 2 .1, the surface roughness was changed by changing the bond strength between mortar matrix and aggregate. It is considered in such specimens that the mechanism of stress transfer to aggregate may be hardly influenced by the surface condition of aggregate. On the other hand, in Exp.-Ⅳ. 2. 2, a material with low elastic modulus was interposed between mortar matrix and aggregate. In such specimens, the stress can not been adequetely transmitted to aggregate.

4. 3. 3. Compressive strength of model concrete

The relations between the compressive strength of model concrete (F_{cc}) and that of aggregate (F_{ca}) obtained by Exp.-Ⅳ. 2 and Exp.-Ⅳ. 3 are plotted in Figs. 4. 7. 1 through 4. 7. 3, in terms of ratios to the compressive strength of mortar matrix (F_{cm}).

(1) Effect of strength of aggregate; Fig. 4. 7. 1 shows the relation between the relative concrete strength (F_{cc}/F_{cm}) and the relative aggregate strength (F_{ca}/F_{cm}) obtained by Exp.-Ⅳ. 2. 1 for N-series specimen with a normal-textured aggregate, R-series specimen with a rough-textured aggregate and P-series specimen with a smooth-textured aggregate. The value of F_{cc}/F_{cm} at $F_{ca}/F_{cm}=0$ in Fig. 4. 7. 1 represents the ratio of the compressive strength of H-series specimen with a cylindrical hole to that of mortar matrix. Fig. 4. 7. 2 shows a similar relation obtained by Exp.-Ⅳ. 3, where, the notations of "MC-MH" and "MC-ML" shown in Fig. 4. 7. 2 represent the specimens having mortar aggregates with $W/C=0.40$ and with $W/C=0.55$, respectively. As indicated in these figures, the compressive strength of model concrete (F_{cc}) closely relates to that of aggregate (F_{ca}). For the specimens with smaller strength of aggregate than that of mortar matrix (in the range of $F_{ca}/F_{cm}<1$), the relative concrete strength (F_{cc}/F_{cm}) increases in proportion to the relative aggregate strength (F_{ca}/F_{cm}). That is to say, the aggregate strength contributes appreciably to the concrete strength in the range of

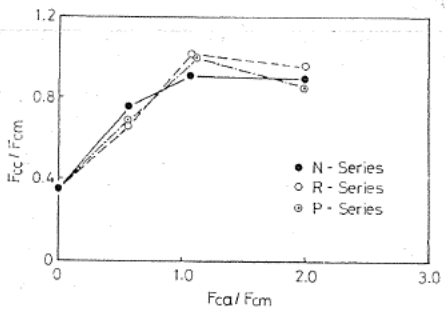

Fig. 4. 7. 1. Exp.-Ⅳ. 2. 1

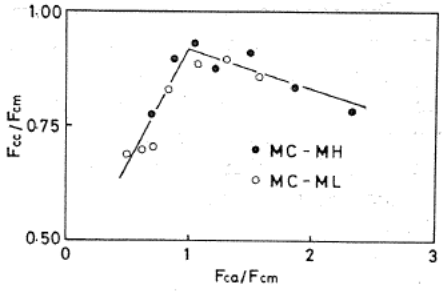

Fig. 4. 7. 2. Exp.-Ⅳ. 3

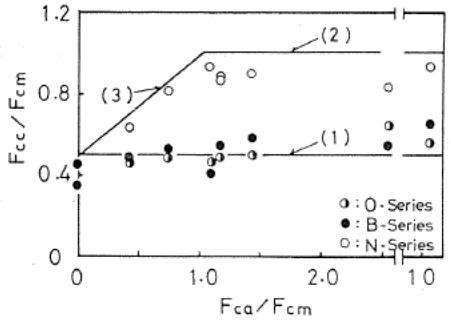

Fig. 4. 7. 3. Exp.-Ⅳ. 2. 2

Fig. 4. 7. Relation between relative concrete strength (F_{cc}/F_{cm}) and relative aggregate strength (F_{ca}/F_{cm}).

$F_{ca}/F_{cm}<1$.

On the other hand, for the specimens with larger strength of aggregate than that of mortar matrix (in the range of $F_{ca}/F_{cm}>1$), the relative concrete strength never increases but slightly decreases with the increase of relative aggregate strength (F_{ca}/F_{cm}). That is to say, aggregate has not a role to strengthen the mortar matrix in the range of $F_{ca}/F_{cm}>1$. As described above, it is noticed that the "law of mixture" is not necessarily existed for the compressive strength of concrete.

The test results of the compressive strength of model concrete can be correlated to the results of the stress-strain behavior described previously. That is, the fracture of specimen with smaller strength of aggregate than that of mortar matrix was caused by the compressive failure in aggregate. Accordingly, it is estimated that the compressive strength of concrete increases with the increase of that of aggregate. On the other hand, the failure of specimen with larger strength of aggregate than that of mortar matrix was caused by the local compressive failure in mortar matrix at the vicinity of aggregate. It is considered in such a case that the stress concentration in mortar matrix increases as the modular ratio of aggregate and mortar matrix (E_a/E_m) or the relative aggregate strength (F_{ca}/F_{cm}) is increased. Accordingly, the compressive strength of concrete appears to decrease with the increase of that of aggregate.

It is of interest to note from the above discussion that the use of larger strength of aggregate than that of mortar matrix is not necessarily efficient for fabricating the high strength concrete.

(2) Effect of surface condition of aggregate

The relation between the relative concrete strength (F_{cc}/F_{cm}) and the relative aggregate strength (F_{ca}/F_{cm}) obtained by Exp.-Ⅳ. 2. 2 is plotted in Fig. 4. 7. 3, together with the previous results.[44] A straight line (1) in Fig. 4. 7. 3 represents the lower limit of F_{cc} which corresponds to the compressive strength of model concrete with a cylindrical hole, and straight lines (2) and (3) represent the upper limits of F_{cc} which correspond to the compressive strength of model concrete with an aggregate bonded perfectly to mortar matrix. The compressive strengths (F_{cc}) of O-series specimen with a bond-reduced aggregate and B-series specimen with a bonded aggregate hardly increase even if the compressive strength of aggregate (F_{ca}) is increased. This fact may be caused by that few amount of stress is transmitted to aggregate, as described previously.

As reported by authors[55] and Nepper-Christensen et al.[64], the compressive strength of concrete made with aggregate coated by a thin layer of paraffin or soft plastic was considerably smaller than that of concrete made with uncoated aggregate. This fact can be explained by the above discussion.

On the other hand, the compressive strength of concrete was not affected by the surface roughness of aggregate as shown in Fig. 4. 7. 1. Let us consider the reason of this fact in more detail.

The mortar failure criterion of Cowan's type[65] and the bond failure criteria between mortar matrix and aggregate obtained by Exp.-Ⅳ. 1. 2 are schematically drawn in Fig. 4. 8. The notations of 60 M, 60 R and 60 N represent Mohr's stress circles for the uniaxial compressive strength of mortar matrix, the shear-compressive bond strength of R-series specimen and that of N-series specimen with W/C $=0.6$, respectively. As shown in Fig. 4. 8, the bond failure occurs at the stress considerably smaller than the compressive strength of mortar, even if the bond strength is fairly improved by increasing the surface roughness of aggregate. Therefore, it will be reasonable to consider that the surface roughness of aggregate will little affect the behavior of concrete after the occurrence of bond crack.

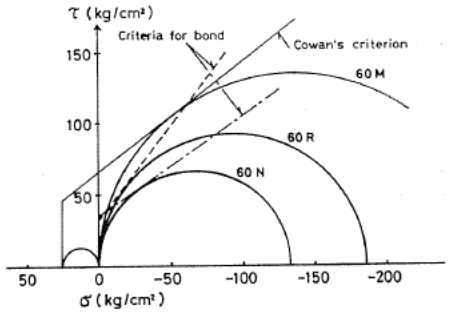

Fig. 4. 8. Schematic failure criteria of mortar matrix and bond at the interface.

Soshiroda et al.[58] have reported that the compressive strength of concrete made with glass ball aggregate was hardly affected by the surface roughness of glass ball. This reason will be explained by the above discussion.

4. 4. Conclusion

In the present chapter, the effect of the mechanical properties and the surface condition of coarse aggregate on the fracture process and the compressive strength of concrete was examined by a model analysis. Summary of this chapter is as follows:

1) The flexual bond strength between mortar matrix and aggregate is not affected by the strength of aggregate but the shear-compressive bond strength between them varies considerably with the strength and the surface condition of aggregate.

2) Bond crack is the first structural change in the model concrete under uniaxial compression, independently of the quality and the surface condition of aggregate used.

3) For model concrete with smaller strength of aggregate than that of mortar matrix, mortar crack and aggregate crack begin to propagate simultaneously after the occurrence of bond crack. Finally, the local compressive failure in aggregate causes the failure of model concrete. Accordingly, the compressive strength of model concrete is greatly influenced by that of aggregate.

4) For model concrete with larger strength of aggregate than that of mortar matrix, mortar crack is interconnected to bond crack and the continuous cracks parallel to the loading axis are formed. Finally, the local compressive failure in mortar matrix at the vicinity of aggregate causes the failure of model concrete. Accordingly, the compressive strength of model concrete is greatly affected by that of mortar matrix.

5) In the range of the relative aggregate strength smaller than 1 ($F_{ca}/F_{cm}<1$), the relative concrete strength (F_{cc}/F_{cm}) increases with the increase of the relative aggregate strength (F_{ca}/F_{cm}), while in the range of $F_{ca}/F_{cm}>1$, the relative concrete strength (F_{cc}/F_{cm}) slightly decreases with the increasing value of F_{ca}/F_{cm}. Accordingly, the use of high-strength aggregate is not necessarily efficient for obtaining the high-strength concrete.

6) The surface roughness of aggregate affects the occurrence of bond crack but hardly affects the compressive strength of model concrete.

5. Concluding Remarks

In the present paper, the effects of the mechanical properties and volume fraction of aggregate and the water-cement ratio of mortar matrix on the mechanism of fracture and failure of concrete as a two-phase composite material were investigated at both the phenomenological and the structural levels. The following three approaches were adopted for the investigation.

At first, the progressive microcracking in concrete was directly observed with a microscope, as described in Chapter 2, and the effects of the type of coarse aggregate and the water-cement ratio of mortar matrix were clarified.

Secondly, the internal fracture process of concrete was indirectly estimated from the aspect of the change of external surface strain, as described in Chapter 3, and the relationships between the characteristic stresses on the stress-strain curve of concrete, such as proportional limit, initiation stress and critical stress, and the progressive microcracking of concrete were clarified.

In the third investigation, i. e., the model analysis described in Chapter 4, the mechanical behavior of model concrete made with mortar matrix and a simple shaped mortar aggregate under uniaxial compression was investigated, and the effects of the strength and surface texture of aggregate on the fracture process and the compressive strength of concrete were clarified.

The results obtained in the above mentioned studies will rather contribute to the better understanding of the mechanism of fracture and failure of concrete as a composite material. However, it is necessary to perform the more experimental

and theoretical investigations for the complete understanding of the mechanism of fracture and failure of concrete under various loading conditions.

(A few applications of test results obtained in Chapter 4 and some theoretical analyses of test results obtained in Chapters 2 and 3 are reported in literature[66]).

Acknowledgement

The authors wish to their sincere gratitude to Messrs. F. Oota, N. Tsuge and K. Kimura for their assistance in the experiments and to Messrs. K. Yamada and Y. Onishi for their typing the manuscript.

References

1) K. Newman, "The Structure and Properties of Concrete-A Introductory Review", Proc. of an International Conference on the Structure of Concrete, London 1965, Cement and Concrete Association, pp.xiii-xxxii.
2) K. Newman, "Composite Materials. Chap. VIII-Concrete Systems", Elsevier Pub. Comp., London 1966, pp. 336-452.
3) H. A. Gillespie, "Concrete Failure-Theory, Mechanism, and Concept", Ph. D. Thesis of Univ. of Arizona, 1968, 253pp.
4) Y. Kondo and S. Ban, "Handbook of Concrete Technology", Asakura Pub. Comp., Tokyo 1965, pp. 275-303 (in Japanese).
5) Y. Kosaka and Y. Tanigawa, "Mechanical Properties of Concrete as a Composite Material", Materials, Jour. of Society of Materials Science of Japan, Vol. **24**, No. 260, May 1975, pp. 368-379 (in Japanese).
6) T. T. C. Hsu, F. O. Slate, G. M. Sturman and G. Winter, "Microcracking of Plain Concrete and the Shape of the Stress-Strain Curve", Jour. of ACI, Vol. **60**, No. 2, Feb. 1963, pp. 209-224.
7) S. P. Shah and F. O. Slate, "Internal Micro-cracking, Mortar-Aggregate Bond and the Stress-Strain Curve of Concrete", Proc. of an International Conference on the Structure of Concrete, London 1965, Cement and Concrete Association, pp. 82-92.
8) G. M. Sturman, S. P. Shah and G. Winter, "Effect of Flexual Strain Gradients on Microcracking and Stress-Strain Behavior of Concrete", Jour. of ACI, Vol. **62**, No. 7, July 1965, pp. 805-822.
9) H. Yokomichi, K. Matsuoka and N. Takada, "Some Experiments on Detection of Crack of Concrete", Cement and Concrete, No. 228, Feb. 1966, pp. 2-6 (in Japanese).
10) T. C. Hansen, "Cracking and Fracture of Concrete and Cement Paste", ACI, SP-20, Detroit, Michigan, 1968, pp. 43-66.
11) K. T. Krishnaswamy, "Strength and Microcracking of Plain Concrete Under Triaxial Compression", Jour. of ACI, Vol. **65**, No. 10, Oct. 1968, pp. 856-862.
12) B. L. Meyers, F. O. Slate and G. Winter, "Relationship Between Time-Dependent Deformation and Microcracking of Plain Concrete", Jour. of ACI, Vol. **66**, No. 1, Jan. 1969, pp. 60-68.
13) S. Popovics, "Fracture Mechanism in Concrete: How much do we know?", Jour. of EM-Div., Proc. of ASCE, Vol. **95**, No. EM3, June 1969, pp. 531-544.
14) S. P. Shah and S. Chandra, "Fracture of Concrete Subjected to Cyclic and Sustained Loading", Jour. of ACI, Vol. **67**, No. 10, Oct. 1970, pp. 816-824.
15) Y. Niwa, W. Koyanagi and K. Nakagawa, "Failure Processes of Concrete Under Triaxial Compressive Stresses", Trans. of Japan Society of Civil Engineers, No. 185, Jan. 1971, pp. 31-41 (in Japanese).
16) K. Kato, "Microcracks and Physical Properties of Plain Concrete", Trans. of Japan Society of Civil Engineers, No. 188, April 1971, pp. 61-72 (in Japanese).

17) A. Yoshimoto and M. Kawakami, "Microcracking in Cement Paste Under Flexure-Tension", Reports of 26th General Meeting of Cement Association of Japan, May 1972, pp. 253-256 (in Japanese).
18) S. Amasaki and T. Akashi, "A Study on the Impact Fatigue Strength of Concrete", Reports of 27 th General Meeting of Cement Association of Japan, May 1973, pp. 253-256 (in Japanese).
19) Y. Kosaka and Y. Tanigawa, "Effect of Aggregate on Fracture Process of Concrete", Reports of Tokai Branch of Architectural Institute of Japan, No. 12, Feb. 1974, pp. 13-16 (in Japanese).
20) Y. Kosaka and Y. Tanigawa, "Effect of Coarse Aggregate on Fracture of Concrete (Part 2: Study on Microscopic Observation)", Trans. of Architectural Institute of Japan, No. 231, May 1975, pp. 1-11 (in Japanese).
21) F. O. Slate and S. Olsefski, "X-Rays for Study of Internal Structure and Microcracking of Concrete", Jour. of ACI, Vol. **60**, No. 3, May 1963, pp. 575-588.
22) G. S. Robinson, "Methods of Detecting the Formation and Propagation of Microcracks in Concrete", Proc. of an International Conference on the Structure of Concrete, London 1965, Cement and Concrete Association, pp. 131-145.
23) T. C. Y. Liu, A. H. Nilson and F. O. Slate, "Stress-Strain Response and Fracture of Concrete in Uniaxial and Biaxial Compression", Jour of ACI, Vol. **69**, No. 5, May 1972, pp. 291-295.
24) R. Jones and M. F. Kaplan, "The Effect of Coarse Aggregate on the Mode of Failure of Concrete in Compression and Flexure", Magazine of Concrete Research, Vol. **9**, No. 26, Aug. 1957, pp. 89-94.
25) R. Jones, "Cracking and Failure of Concrete Test Specimens under Uniaxial Quasi-static Loading", Proc. of an International Conference on the Structure of Concrete, London 1965, Cement and Concrete Association, pp. 125-130.
26) H. Kawakami, "Effect of Size and Quantity of Aggregate on Compressive Strength of Concrete", Trans. of Architectural Institute of Japan, No. 186, Aug. 1971, pp. 1-11 (in Japanese).
27) K. Kato, "Microcracks and Evaluation of Mechanical Properties of Plain Concrete", Trans. of Japan Society of Civil Engineers, No. 208, Dec. 1972, pp. 121-136 (in Japanese).
28) R. L'Hermite, "Recent Day Ideas on Concrete Technology. 3rd Part-The Failure of Concrete", RILEM Bulletin, No. 18, June 1954, pp. 27-39.
29) H. Rüsch, "Physical Problems in the Testing of Concrete", Zement-Kalk-Gips, Vol. **13**, 1959, pp. 1-9.
30) F. E. Richart, A. Brandtzaeg and R. L. Brown, "The Failure of Plain and Spirally Reinforced Concrete in Compression", Univ. of Illinois Eng. Expt. Station, Bulletin No. 190, April 1929.
31) M. F. Kaplan, "Strains and Stresses of Concrete at Initiation of Cracking and Near Failure", Jour. of ACI, Vol. **60**, No. 7, July 1963, pp. 853-880.
32) P. Desayi and P. S. Viswanatha, "True Ultimate Strength of Plain Concrete", RILEM Bulletin, No. 36, Sept. 1967, pp. 163-173.
33) L. Béres, "Investigation on Structural Loosening of Compressed Concrete". RILEM Bulletin, No. 36, Sept. 1967, pp. 185-190.
34) S. P. Shah and S. Chandra, "Critical Stress, Volume Change, and Microcracking of Concrete", Jour. of ACI, Vol. **65**, No. 9, Sept. 1968, pp. 770-781.
35) H. Yokomichi, Y. Kakuta and K. Ayuta, "On Critical Points in Deformation of Concrete", Reports of 23rd General Meeting of Cement Association of Japan, May 1969, pp. 231-235 (in Japanese).
36) H. Yokomichi, Y. Kakuta and S. Terasawa, "Critical Points of Deformation and Cracking of Concrete", Reports of 24 th General Meeting of Cement Association of Japan, May 1970, pp. 282-285 (in Japanese).
37) H. Okamoto and K. Yamamoto, "On the Internal Cracking of Lightweight Concrete", Reports of 25th General Meeting of Cement Association of Japan, June 1971, pp. 296-300

(in Japanese).
38) S. Hasaba, M. Kawamura, K. Miyakita and M. Saito, "Study on Poisson's Ratio and Microcrack Extension in High Strength Concrete", Reports of 26 th General Meeting of Cement Association of Japan, May 1972, pp. 283-287 (in Japanese).
39) Y. Kosaka and Y. Tanigawa. "Critical Stress of Mortar and Concrete Made of Various Aggregates", Reports of 27 th General Meeting of Cement Association of Japan, May 1973, pp. 238-242 (in Japanese).
40) Y. Kosaka and Y. Tanigawa, "Effect of Aggregate on Fracture of Concrete (Part 3: Study on Stress-Strain Curve of Concrete)", Trans. of Architectural Institute of Japan, No. 233, July 1975, pp. 21-32 (in Japanese).
41) M. Okushima, K. Suzuki and T. Nakatsuka, "The Experimental Study on Mechanical Properties of Concrete Having Model Coarse Aggregate", Reports of 27th General Meeting of Cement Association of Japan, May 1973, pp. 207-211 (in Japanese).
42) A. Yoshimoto and M. Kawakami, "Relation Between Particular Points in Deformation Behavior of Concrete and Microcracking", Reports of 28th General Meeting of Cement Association of Japan, May 1974, pp. 234-237 (in Japanese).
43) S. P. Shah and G. Winter, "Inelastic Behavior and Fracture of Concrete", ACI, SP-20, Detroit, Michigan, 1968, pp. 5-28.
44) Y. Kosaka, Y. Tanigawa and F. Oota, "Effect of Aggregate-Matrix Interaction on Mechanical Properties of Concrete", Proc. of 15th Japan Congress on Materials Research, Sept. 1971, pp. 64-68.
45) Y. Kosaka, Y. Tanigawa and F. Oota, "Effect of Coarse Aggregate on Fracture of Concrete (Part 1: Model Analysis)", Trans. of Architectural Institute of Japan, No. 228, Feb. 1975, pp. 1-11 (in Japanese).
46) T.Shiire and Y. Oomagari, "Bond Behavior Between Aggregate and Mortar at Failure of Concrete", Abstracts of Trans. of Architectural Institute of Japan, Oct. 1972, pp. 31-32 (in Japanese).
47) Johoji and K. Kato, "Strain Distribution in Plain Concrete", Memoirs of the Defense Academy, Japan, Vol. **VII**, No. 3, 1957, pp. 1135-1146.
48) H. D. Fein, "Spannungszustand in Modelbetonen bei einachsiger Druck-und zweiachsiger Druck-Zug-Beanspruchung", Universität Karlsruhe, 1971.
49) O. Buyukozturk, A. H. Nilson and F. O. Slate, "Stress-Strain Response and Fracture of Concrete Model in Biaxial Loading", Jour. of ACI, Vol. **68**, No. 8, Aug. 1971, pp. 590-599.
50) Y. Kosaka, Y. Tanigawa and F. Oota, "Mechanical Properties of Concrete Made with Model Aggregate", Abstracts of Trans. of Architectural Institute of Japan, Oct. 1972, pp. 45-48 (in Japanese).
51) Y. Kosaka, Y. Tanigawa and F. Oota, "Effect of Aggregate Interaction on Mechanical Properties of Concrete", Reports of 27 th General Meeting of Cement Association of Japan, May 1973, pp. 212-216 (in Japanese).
52) M. Okushima, K. Suzuki and T. Nakatsuka, "Failure of Model Concrete", Abstracts of Trans. of Architectural Institute of Japan, Oct. 1972, pp. 33-34 (in Japanese).
53) G. Wischers and M. Lusche, "Einfluss der inneren Spannungsverteilung auf das Tragverhalten von druckbeanspruchtem Normal-und Leichtbeton", Beton, Aug. 1972, pp. 343-347: Sept. 1972, pp. 397-403.
54) T. Okajima, "The Mechanical Properties of Particulate Composites under Static Compression", Trans. of Architectural Institute of Japan, No. 176, Oct. 1970, pp. 1-10 (in Japanese).
55) Y. Kosaka, Y. Tanigawa and F. Oota, "Compressive Strength of Concrete with Cubic Aggregate of Cement Mortar", Materials, Jour. of Society of Materials Science of Japan, Vol. **20**, No. 208, Jan. 1971, pp. 41-46 (in Japanese).
56) J. E. Ash, "Bleeding in Concrete-A Microscopic Study", Jour. of ACI, Vol. **69**, No. 4, April 1972, pp. 209-211.
57) Y. Kosaka, Y. Tanigawa and F. Oota, "Effect of Bond Between Coarse Aggregate and Mortar Matrix on Mechanical Properties of Concrete", Reports of 26 th General Meeting

of Cement Association of Japan, May 1972, pp. 278-282.
58) T. Soshiroda, K. Fujisawa and T. Ikawa, "Study on Anisotropy of Concrete (VII)-Effect of Coarse Aggregate", Abstracts of Trans. of Architectural Institute of Japan, Oct. 1973, pp. 375-376 (in Japanese).
59) A. Brandtzaeg, "Failure of Material Composed of Non-Isotropic Elements", Det Kongelige Norske Videnskabernes Selskabs Skrifter, No. 2, Trondheim, 1927, p. 68.
60) E. Reinius, "A Theory of the Deformation and the Failure of Concrete", Magazine of Concrete Research, Vol. 8, No. 24, Nov. 1956, pp. 157-160.
61) A. L. L. Baker, "An Analysis of Deformation and Failure Characteristics of Concrete", Magazine of Concrete Research, Vol. 11, No. 33, Nov. 1959, pp. 119-128.
62) M. Anson, "An Investigation Into a Hypothetical Deformation and Failure Mechanism for Concrete", Magazine of Concrete Research, Vol. 16, No. 47, June 1964, pp. 73-82.
63) D. Darwin and F. O. Slate, "Effect of Paste-Aggregate Bond Strength on Behavior of Concrete", Jour. of Materials, Vol. 5, No. 1, March 1970, pp. 86-98.
64) P. Nepper-Christensen and T. P. H. Nielsen, "Modal Determination of the Effect of Bond Between Coarse Aggregate and Mortar on the Compressive Strength of Concrete", Jour. of ACI, Vol. 66, No. 1, Jan. 1969, pp. 69-72.
65) H. J. Cowan, "The Strength of Plain, Reinforced and Prestressed Concrete Under the Action of Combined Stress", Magazine of Concrete Research, Vol. 5, No. 14, Dec. 1953, pp. 75-86.
66) Y. Kosaka and Y. Tanigawa, "Mechanical Characteristics of Artificial Lightweight Aggregate Concrete", Trans. of Architectural Institute of Japan, No. 240, Feb. 1976, pp. 21-29 (in Japanese).